Functionally and structurally distinct fusiform face area(s) in over 1000 participants

Xiayu Chen[1,2], Xingyu Liu[1], Benjamin J. Parker[3], Zonglei Zhen[1,2], Kevin S. Weiner[3,4]

1. *Faculty of Psychology, Beijing Normal University, China*
2. *State Key Laboratory of Cognitive Neuroscience and Learning, Beijing Normal University, China*
3. *Helen Wills Neuroscience Institute, University of California Berkeley, USA*
4. *Psychology Department, University of California Berkeley, USA*

Corresponding author

Zonglei Zhen, Ph.D., Faculty of Psychology, Beijing Normal University, Beijing, 100875, China, zhenzonglei@bnu.edu.cn

Acknowledgments: This research was supported by a T32 HWNI training grant (BJP), a NICHD R21HD100858 (KSW and SAB), an NSF CAREER Award 392 2042251 (KSW), and a National Natural Science Foundation of China 31771251 (ZZ). Data were provided by the Human Connectome Project, WU-Minn Consortium (Principal Investigators: David Van Essen and Kamil Ugurbil; 1U54MH091657) funded by the 16 NIH Institutes and Centers that support the NIH Blueprint for Neuroscience Research; and by the McDonnell Center for Systems Neuroscience at Washington University.

Conflict of Interest: The authors declare no competing financial interests.

ABSTRACT

The Fusiform Face Area (FFA) is a widely studied region causally involved in face perception. Even though cognitive neuroscientists have been studying the FFA for over two decades, answers to foundational questions regarding the structure, function, and connectivity of the FFA from a large (N>1000) group of participants are still lacking. To fill this gap, we quantified structural, functional, and connectivity features of fusiform face-selective regions in 1080 participants in the Human Connectome Project (HCP). After manually defining over 4,000 fusiform face-selective regions, we report five main findings. First, 68.94% of hemispheres have two cortically separate regions (pFus-faces/FFA-1 and mFus-faces/FFA-2). Second, in 26.48% of hemispheres, pFus-faces/FFA-1 and mFus-faces/FFA-2 are spatially contiguous, yet functionally and structurally distinct. Third, pFus-faces/FFA-1 is more face-selective than mFus-faces/FFA-2, and the two regions have distinct functional connectivity fingerprints. Fourth, pFus-faces/FFA-1 is cortically thinner and more heavily myelinated than mFus-faces/FFA-2. Fifth, face-selective patterns and functional connectivity fingerprints of each region were more similar in monozygotic than dizygotic twins and more so than structural gradients. As we share our areal definitions with the field, future studies can explore how structural and functional features of these regions will inform theories regarding how visual categories are represented in the brain.

INTRODUCTION

Determining how visual categories are represented in the brain continues to be a major goal and a highly debated topic in cognitive neuroscience with many different proposed theories (Apurva et al., 2004; Behrmann & Plaut, 2013; Grill-Spector & Weiner, 2014; Haxby et al., 2001, 2011; Huth et al., 2012, 2016; Kanwisher, 2000, 2010; Kriegeskorte et al., 2008; Mahon & Caramazza, 2009; Malach et al., 2002; Martin, 2007; McGugin et al., 2012; Pitcher & Ungerleider, 2021; Tarr & Gauthier, 2000). Theoretical debates aside – for example, the ever-popular arguments between modular vs. distributed processing (Haxby et al., 2000, 2001, 2011; Kanwisher et al., 1997; Kanwisher, 2000, 2010), as well as the role of expertise (Gauthier et al., 1999, 2000; McGugin et al., 2012; Tarr & Gauthier, 2000) in the importance, emergence, and function of clustered and distributed category representations in ventral temporal cortex (VTC) – there is great interest in cortical networks selective for faces across species (Arcaro et al., 2019; Bell et al., 2011; Grill-Spector et al., 2017; Nasr et al., 2011; Pinsk et al., 2009; Silson et al., 2016, 2018; Tsao et al., 2008; Tsao & Livingstone, 2008). In humans, the Fusiform Face Area (FFA; Kanwisher et al., 1997; Kanwisher, 2010) is a widely studied functional region located in VTC that is causally involved in face perception (Jonas et al., 2018; Jonas & Rossion, 2021; Parvizi et al., 2012; Rangarajan et al., 2014; Schalk et al., 2017). Nevertheless, even though the extended field has been studying the FFA for over two decades and despite great interest in the FFA in development (Cohen et al., 2019; Deen et al., 2017; Golarai et al., 2007; Gomez et al., 2017; Grill-Spector et al., 2008; Scherf et al., 2007, 2012, 2014), ageing (Park et al., 2012), and among patient populations (Avidan

& Behrmann, 2021; Duchaine & Yovel, 2015; Golarai et al., 2010; Jonas & Rossion, 2021; Maher et al., 2019; Rossion, 2008; Rossion et al., 2003, 2018; Schalk et al., 2017), we still lack answers to foundational questions regarding the structure, function, and connectivity of the FFA from a large (N>1000) group of participants with analyses at the level of individual subjects.

These gaps in knowledge persist for two main reasons. First, most human brain imaging studies perform analyses at the group level in which data are collapsed across participants and analyzed in volume space (previously referred to as "traditional neuroimaging methods"; Coalson et al., 2018). However, group-level functional maps often do not match the functional organization in individual participants. In fact, a recent review paper used the FFA as an example to illustrate this mismatch (Van Essen & Glasser, 2018). Second, studies performing analyses within individual participants manually define the FFA in each hemisphere, which while an arduous process, is still the most accurate method for defining functional regions in individual participants – even for primary sensory areas given recent findings (Benson et al., 2021) – compared to automated approaches. Consequently, given this manual and labor-intensive process, many studies interested in face processing at the level of individual participants suffer from relatively small sample sizes (typically in the ballpark between 10 and 50 participants; Çukur et al., 2013; Davidenko et al., 2012; Downing et al., 2006; Elbich & Scherf, 2017; Engell & McCarthy, 2013; Finzi et al., 2021; Gomez et al., 2015, 2017, 2018; Grill-Spector et al., 2004; Julian et al., 2012; Kay et al., 2015; Kietzmann et al., 2012; McGugin et al., 2014, 2015, 2016; Natu et al., 2016, 2019; Nordt et al., 2021; Parvizi et al., 2012; Pitcher et al., 2011; Rosenke et al., 2020, 2021; Scherf et al., 2017; Stigliani et al., 2015, 2019;

Weiner et al., 2010, 2014, 2016, 2017; Weiner & Grill-Spector, 2010; countless others) because manually defining functional regions is time consuming.

Here, we fill these gaps in knowledge by quantifying structural, functional, and connectivity features of fusiform face-selective regions in 1080 participants included in the Human Connectome Project (HCP). To do so, we implemented a four-fold approach. First, we manually identified fusiform face-selective regions in all 2,160 hemispheres to determine incidence rates regarding how often a participant will have 0, 1, or 2 face-selective regions in either left or right hemisphere in a large group of participants for the first time. Second, we extracted macroanatomical (cortical thickness) and microstructural (myelination) features of each region. Third, we quantified functional (face selectivity) and connectivity (resting-state functional connectivity) features of each region. Fourth, we examined the similarity in spatial patterns of each structural, functional, and connectivity feature between pairs of monozygotic (MZ) and dizygotic (DZ) twins included in the HCP dataset.

Our study revealed five main findings. First, 68.94% of hemispheres have two cortically separate face-selective regions. Second, in 26.48% of hemispheres, pFus-faces/FFA-1 and mFus-faces/FFA-2 were identifiable and contiguous, but could be separated based on anatomical criteria (Weiner, 2019; Weiner et al., 2014). Third, in both the contiguous and separate groups, pFus-faces/FFA-1 was more face-selective than mFus-faces/FFA-2, and the two regions also had distinct functional connectivity fingerprints. Fourth, pFus-faces/FFA-1 in the posterior FG was cortically thinner and more heavily myelinated than the more anterior mFus-faces/FFA-2. Fifth, face-selective

patterns and functional connectivity fingerprints of each region were more similar in MZ than DZ twins and more so than structural gradients of thickness and myelination.

Altogether, we show that pFus-faces/FFA-1 and mFus-faces/FFA-2 are dissociable based on functional, macroanatomical, microstructural, and connectivity features in over 1000 participants for the first time. As we share our areal definitions with the field (http://www.brainactivityatlas.org/atlas/atlas-download), future studies can perform novel multimodal analyses that leverage the rich multimodal HCP dataset to explore how structural and functional features of these regions relate to cognitive and behavioral metrics also acquired in each participant. Finally, to our knowledge, these results provide the first empirical modification of an area within the recently proposed multimodal map of the human cerebral cortex ("FFC" from Glasser et al., 2016) – importantly, this modification is at the level of individual participants, which we share with the field.

RESULTS

95.42% of hemispheres have two face-selective regions on the FG

We manually delineated face-selective regions on the lateral aspect of the fusiform gyrus (FG) in 1080 participants from the HCP and determined incidence rates regarding how often a hemisphere had 0, 1, or 2 FG face-selective regions in a large group of participants for the first time. At least one face-selective region, or "Fusiform Face Area" (FFA), was identifiable in every hemisphere in each participant and 95.42% of hemispheres had two face-selective regions on the FG. The spatial organization of FG face-selective regions could be categorized into one of three different types, or topological groups, in a given hemisphere: separate, continuous, or single. A majority of hemispheres belonged to the separate group in which 68.94% of hemispheres (left hemisphere [LH]: 72.31%; right hemisphere [RH]: 65.56%) contained two face-selective regions that were separated by a cortical gap of several millimeters (Fig. 1B, top). In the continuous group, which consisted of 26.48% of cases (LH: 23.24%; RH: 29.72%), mFus-faces/FFA-2 and pFus-faces/FFA-1 were identifiable and contiguous, but could be separated based on previously proposed anatomical criteria based on cortical folding (Fig. 1B, middle). Specifically, mFus-faces/FFA-2 was identified as the functional region located adjacent to the anterior tip of the mid-fusiform sulcus (MFS), while pFus-faces/FFA-1 was identified as the functional region located adjacent to the posterior extent of the MFS extending into the lateral FG and nearby occipito-temporal sulcus (Weiner, 2019; Weiner et al., 2014). In the single group, which consisted of less than 5% of cases (LH: 4.44%; RH: 4.72%),

either mFus-faces/FFA-2 or pFus-faces/FFA-1, but not both, was identifiable in a given hemisphere based on the criteria just described (Fig. 1B, bottom).

In the continuous and separate groups, there was a 2.27 centimeter cortical gap that separated (on average) the most face-selective vertex from pFus-faces/FFA-1 and that from mFus-faces/FFA-2 (Fig. 1C), measured by the geodesic distance. A 2-way between-subject ANOVA with hemisphere (LH, RH) and group (continuous, separate) as factors revealed that the distance increased when two cortically separate regions were present ($F(1, 2057)=431.66$, $p<.001$). Furthermore, the distance between the most selective vertices was larger in the LH compared to the RH within the separate group ($F(1, 2057)=17.26$, $p<.001$), but not within the continuous group ($F(1, 2057)=.18$, $p=.671$). Additionally, within the separate group, there was a 0.59 centimeter cortical gap (on average) between mFus-faces/FFA-2 and pFus-faces/FFA-1 (Fig. 1D; measured by the minimum distance between the vertices of the two regions). This cortical gap was larger in the LH than that in the RH ($t(1487)=9.22$, $p<.001$), which supports previous qualitative observations in a much smaller sample size (N=7; Weiner and Grill-Spector, 2010).

The surface area differences in FG face-selective regions were also revealed by a 3-way between-subject ANOVA with hemisphere (LH, RH), group (single, continuous, separate), and region (pFus-faces/FFA-1, mFus-faces/FFA-2) as factors (Fig. 1E). Specifically, pFus-faces/FFA-1 was slightly larger in both hemispheres compared to mFus-faces/FFA-2 within the continuous ($F(1, 4209)=4.04$, $p=.045$) and separate groups ($F(1, 4209)=4.16$, $p=.041$), but not the single group ($F(1, 4209)=1.10$, $p=.294$). Moreover, both regions were larger in the RH compared to the LH across the three groups ($F(1, 4209)=12.11$, $p=.001$).

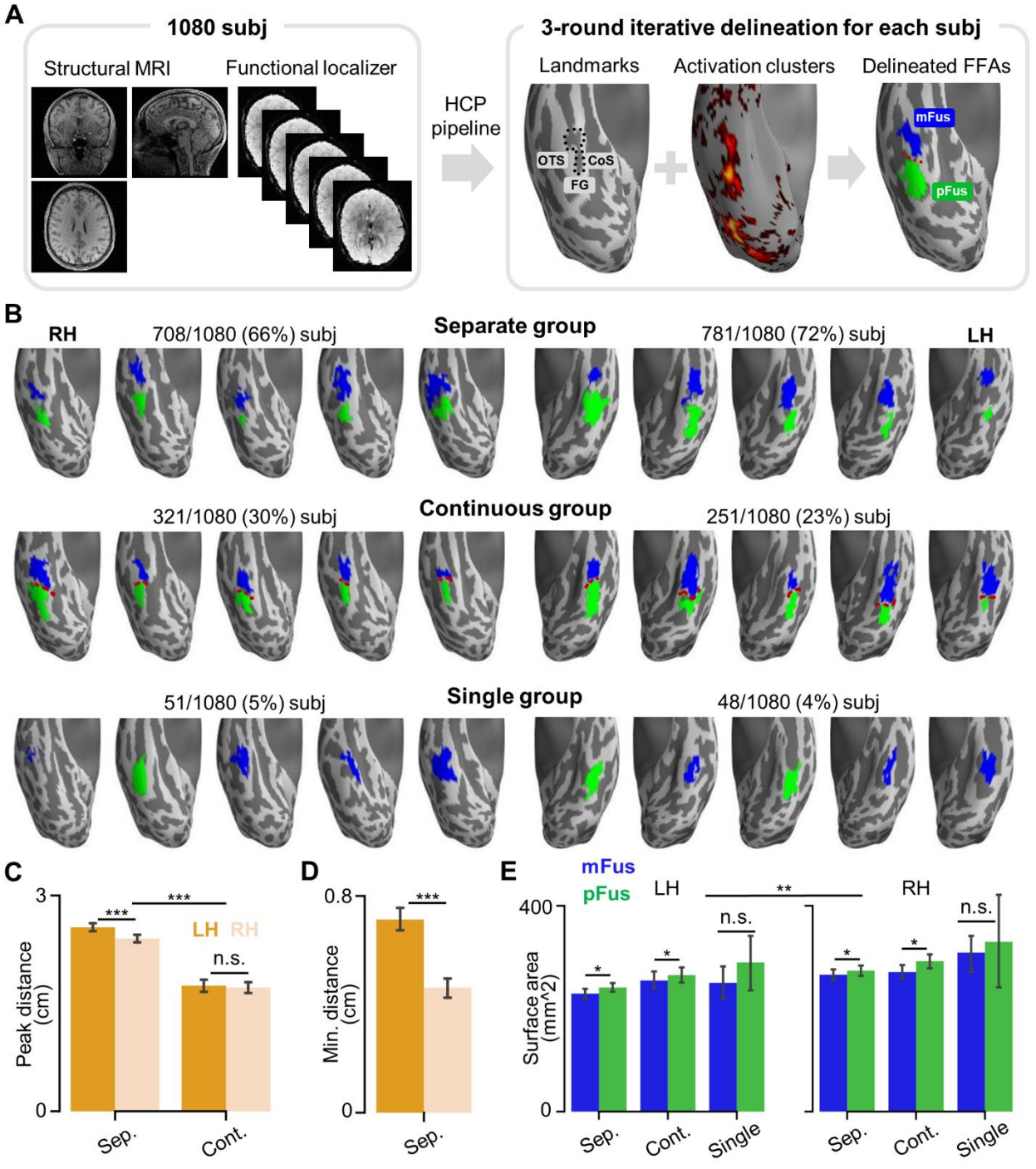

Figure 1. Three topological groups of face-selective regions on the lateral fusiform gyrus (FG) in over 1000 participants. (A) Face-selective regions were manually delineated on the lateral aspect of the fusiform gyrus (FG) in 1080 participants from the HCP using structural (left) and functional (right) data. By taking both individual cortical landmarks (OTS: occipito-temporal sulcus; CoS: collateral sulcus; MFS: mid-fusiform sulcus (black dotted line)) and face-selective activation clusters (faces versus others, Z>1.65, p<0.05, uncorrected) into account, face-selective regions were labeled as

either mFus-faces/FFA-2 or pFus-faces/FFA-1 in each hemisphere based on previously published criteria differentiating the cortical location of these two regions. Specifically, pFus-faces/FFA-1 is located adjacent to the posterior extent of the MFS extending into the lateral FG and the nearby OTS, while mFus-faces/FFA-2 is located adjacent to the anterior tip of the MFS. A three round iterative delineation procedure was implemented for the definition of face-selective regions in each hemisphere (Materials and Methods). (B) Face-selective regions are depicted from 30 randomly chosen hemispheres (5 for each hemisphere and each group). Top row: separate group; Middle row: continuous group; Bottom row: single group. Incidence rates are included above each row for the RH and LH, respectively. (C) Cortical distance between the most face-selective vertices of the two face-selective regions in separate and continuous groups. (D) Cortical gap between the two face-selective regions in the separate group, calculated as the minimum distance between them. (E) Surface areas of individual face-selective regions within the three groups. Error bars indicate the 95% confidence interval; *p<0.05; **p<0.01; ***p<0.001; n.s., not significant. LH: left hemisphere; RH: right hemisphere.

The spatial distribution of face-selective regions is stable across groups, while pFus-faces/FFA-1 is more face-selective than mFus-faces/FFA-2

A group-specific probabilistic map was created for each FG face-selective region in each group (Fig. 2A), which provided a vertex-wise description for the spatial distribution of each region. We found that both FG face-selective regions showed high spatial consistency across groups in both hemispheres (Fig. 2B). Specifically, the Pearson correlation coefficients between probabilistic maps from the separate and continuous groups are greater than 0.95. As expected, the spatial consistency between the single group and either the continuous or separate group was lower because the probabilistic maps of the single group suffered from smaller sample sizes.

After characterizing the stability of pFus-faces/FFA-1 and mFus-faces/FFA-2, we next tested if there were differences in face selectivity between the two regions. As pFus-faces/FFA-1 and mFus-faces/FFA-2 are defined based on the HCP working memory task, we used face and shape conditions from the emotional processing task, which was also

included in the HCP dataset, as an independent dataset to compare face selectivity between the two face-selective regions in each of the three groups. Crucially, these data were acquired in nearly all participants and completely independent from the data used to define each face-selective region. We found that pFus-faces/FFA-1 is more face-selective than mFus-faces/FFA-2, as well as differences across groups (Fig. 2C). Specifically, a 3-way between-subject ANOVA with hemisphere (LH, RH), group (single, continuous, separate), and region (pFus-faces/FFA-1, mFus-faces/FFA-2) as factors revealed a hemisphere x group x region interaction ($F(2, 3665)=3.08$, $p=.046$), which is largely driven by the single (region x hemisphere interaction: $F(1, 75)=5.10$, $p=.027$) and continuous (region x hemisphere interaction ($F(1, 992)=4.94$, $p=.026$) groups. In addition, there was also a region x group interaction in the right hemisphere ($F(2, 1829)=8.91$, $p<.001$). Further, we found that pFus-faces/FFA-1 is more face-selective than mFus-faces/FFA-2 for the continuous and separate groups in both hemispheres (all Fs$(1, 3665)>=52.11$; all ps$<.001$).

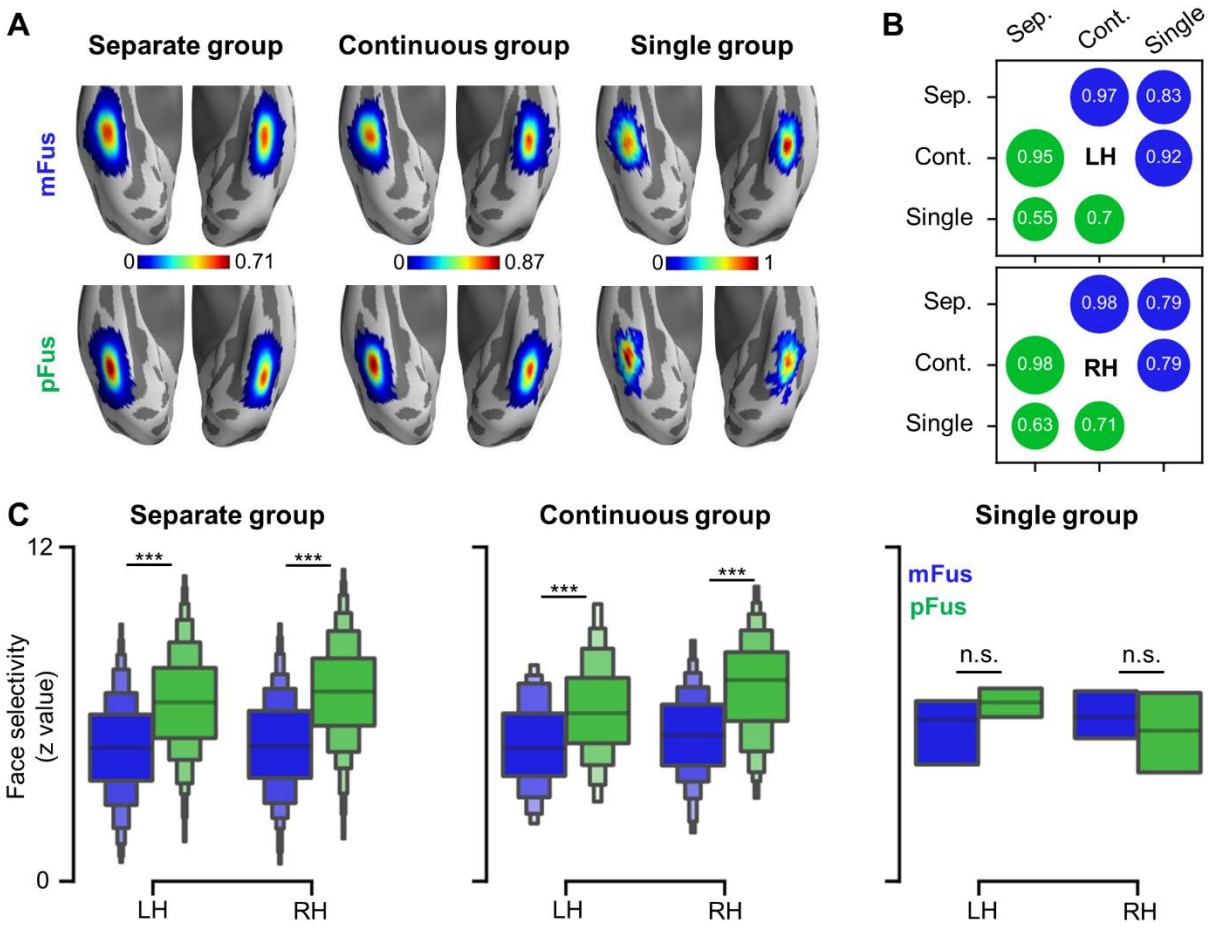

Figure 2. Spatial distribution and face selectivity of fusiform face-selective regions. (A) Probabilistic maps of face-selective regions in the three groups (separate, continuous, single). Top row: mFus-faces/FFA-2; Bottom row: pFus-faces/FFA-1. (B) Both face-selective regions showed high spatial consistency across groups in both hemispheres, measured by the Pearson correlation coefficient between the probabilistic maps of each pair of groups. The spatial consistency between the single group and either the continuous or separate group was lower because the probabilistic maps of the single group suffered from smaller sample sizes (Figure 1 and Results for incidence rates). Blue circle: mFus-faces/FFA-2; Green circle: pFus-faces/FFA-1. (C) pFus-faces/FFA-1 (green) is more face-selective than mFus-faces/FFA-2 (blue) in both the separate and continuous groups, but not the single group. ***p<0.001; n.s., not significant. LH: left hemisphere; RH: right hemisphere.

mFus-faces/FFA-2 is cortically thicker and less myelinated than pFus-faces/FFA-1

Are there structural differences between pFus-faces/FFA-1 and mFus-faces/FFA-2 that could serve as underlying anatomical substrates for the functional differences

between these two regions? Two complementary approaches from previous research suggests that pFus-faces/FFA-1 and mFus-faces/FFA-2 are likely macroanatomically and microstructurally distinct from one another. First, previous research showed that microstructurally, pFus-faces/FFA-1 and mFus-faces/FFA-2 are located in different cytoarchitectonic territories (Gomez et al., 2018; Weiner et al., 2017). Second, additional work showed that cytoarchitectonic regions early in the visual processing hierarchy were cortically thinner and more myelinated than cytoarchitectonic regions positioned later in the visual processing hierarchy in which the expression of a sparse subset of genes contributed to these differences (Gomez et al., 2019). However, these studies combined data from living and post-mortem individuals to draw these conclusions. Thus, building on these previous findings, we tested if pFus-faces/FFA-1 and mFus-faces/FFA-2 were anatomically distinct by calculating average macroanatomical (e.g., cortical thickness) and microstructural (e.g., myelination) values from each region in each individual participant for the first time.

This approach revealed that mFus-faces/FFA-2 is cortically thicker and less myelinated than pFus-faces/FFA-1, but only when two face-selective regions on the FG are present (Fig. 3). Specifically, a 4-way between-subject ANOVA with metric (myelination, thickness), hemisphere (LH, RH), group (single, contiguous, separate), and region (pFus-faces/FFA-1, mFus-faces/FFA-2) as factors revealed a metric × region interaction ($F(1,8418)=160.67$, $p<.001$). This interaction is driven by the fact that pFus-faces/FFA-1 is more myelinated than mFus-faces/FFA-2 across groups ($F(1,8418)=5.35$, $p=.021$) and mFus-faces/FFA-2 is cortically thicker than pFus-faces/FFA-1 across groups ($F(1,8418)=243.76$, $p<.001$).

As illustrated in Fig. 3A, a separate 3-way between-subject ANOVA with hemisphere (LH, RH), group (single, contiguous, separate), and region (pFus-faces/FFA-1, mFus-faces/FFA-2) as factors showed an interaction in which when either mFus-faces/FFA-2 or pFus-faces/FFA-1 was present (but not both; Fig. 3A, right)), there was no difference in myelin content ($F(1,4209)=.57$, $p=.450$), while for the continuous and separate groups, pFus-faces/FFA-1 had more myelin content than mFus-faces/FFA-2 (all Fs$(1,4209)>514.32$; all ps$<.001$; Fig. 3A, left, middle). Finally, we also found different degrees of myelination among the three groups for mFus-faces/FFA-2 ($F(2, 4209)=23.93$, $p<.001$) and for pFus-faces/FFA-1 ($F(2, 4209)=5.76$, $p=.003$), indicating that the spatial organization of face-selective regions on the FG also indicates individual differences in the underlying anatomy related to network connectivity such as the amount of myelination on the FG.

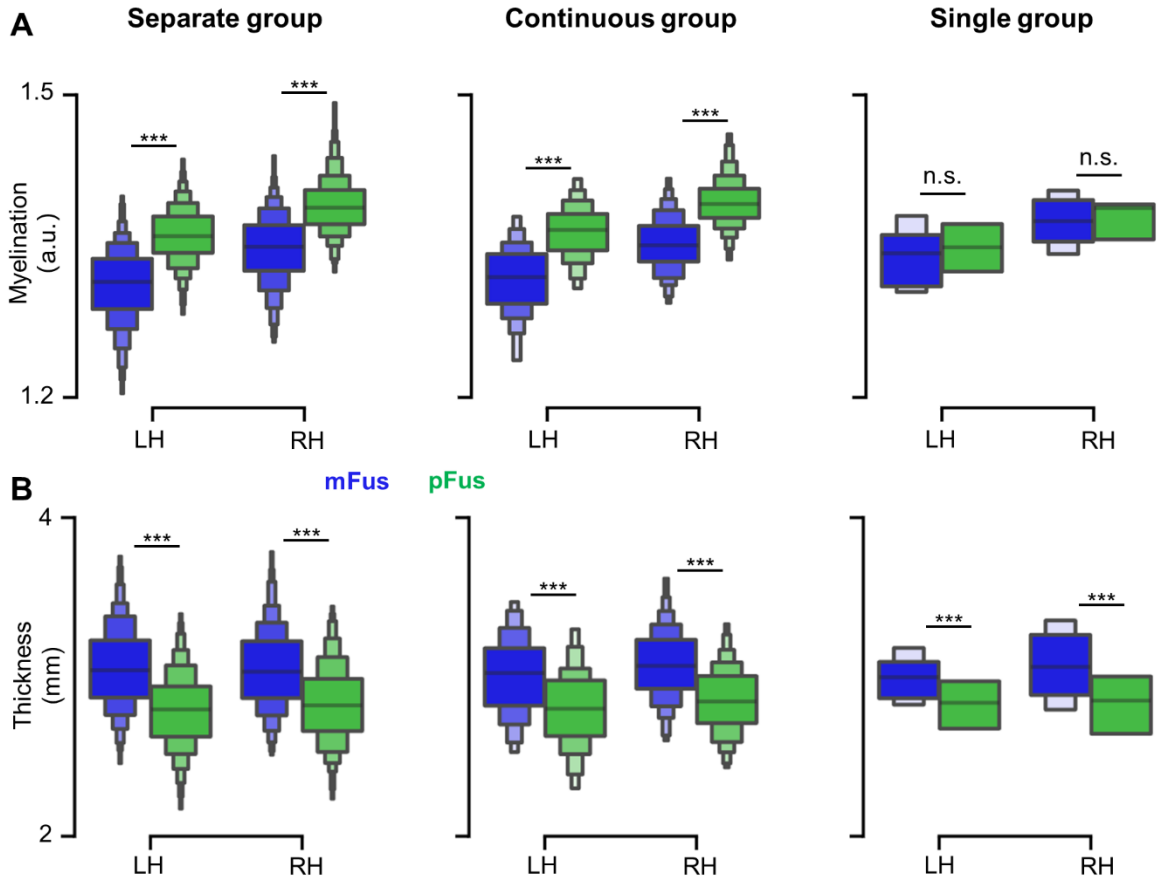

Figure 3. mFus-faces/FFA-2 is cortically thicker and less myelinated than pFus-faces/FFA-1. (A) pFus-faces/FFA-1 (green) has a higher myelin content than mFus-faces/FFA-2 (blue) in the separate and continuous groups, but not the single group. (B) mFus-faces/FFA-2 (blue) is cortically thicker than pFus-faces/FFA-1 (green) across groups. ***p<0.001; n.s., not significant. LH: left hemisphere; RH: right hemisphere.

mFus-faces/FFA-2 and pFus-faces/FFA-1 have different functional connectivity "fingerprints"

To quantify potential functional connectivity differences between these two face-selective regions, we considered three scales: i) areal, ii) network, and iii) global. At the areal level, we quantified the intrinsic resting-state functional connectivity (RSFC) between face-selective regions and regions from the multimodal parcellation (MMP) of the human cerebral cortex by Glasser and colleagues (2016). We found that pFus-

faces/FFA-1 was more strongly connected to a majority of regions compared to mFus-faces/FFA-2 in both continuous and separate groups (all *t*s>2.05, *p*s<.046, FDR corrected; Fig. 4A), but not in the single group (all *t*s<2.82, all *p*s>.990, FDR corrected). Furthermore, we found that mFus-faces/FFA-2 was more strongly connected to a small number of regions compared to pFus-faces/FFA-1 with an effect of group. In the continuous group, mFus-faces/FFA-2 had stronger functional connectivity with ipsilateral TF and TE2p (Fig. S1-S2; all *t*s<4.09, all *p*s<.001, FDR corrected). In the separate group, left mFus-faces/FFA-2 was more strongly connected to anterior temporal (L_TF, L_TE2p), orbitofrontal (L_47m), anterior cingulate (R_25, L_25), posterior cingulate (L_v23ab), and lateral parietal (L_PGs) cortices (Fig. S3; all *t*s<2.19, all *p*s<.035, FDR corrected), while right mFus-faces/FFA-2 was only more strongly connected to area R_TF (Fig. S4; *t*=13.39, *p*<.001, FDR corrected).

At the network level, the RSFCs of all MMP areas were summarized into 12-dimension RSFC “fingerprints” according to Cole-Anticevic Brain Network Parcellation (CAB-NP) (Ji et al., 2019). This approach revealed that in participants within the single group, there was no difference in the connectivity fingerprints between pFus-faces/FFA-1 and mFus-faces/FFA-2 in both hemispheres (all *t*s<1.67, all *p*s>.85, FDR corrected), while these fingerprints were functionally distinct from one another when two regions were present (Fig. 4B, scatter plot). Specifically, in the continuous group, pFus-faces/FFA-1 showed stronger RSFC than mFus-faces/FFA-2 to all networks with the exception of the default mode and the ventral multimodal networks (all *t*s>2.62, all *p*s<.011, FDR corrected). In the separate group, pFus-faces/FFA-1 showed stronger RSFC than mFus-faces/FFA-2 to all networks with the exception of the default mode in the LH (all *t*s>5.93,

all *p*s<.001, FDR corrected) and of the ventral multimodal networks in both hemispheres (all *t*s>2.75, all *p*s<.006, FDR corrected). mFus-faces/FFA-2 showed stronger RSFC than pFus-faces/FFA-1 only in the ventral multimodal network (all *t*s<3.43, all *p*s<.001, FDR corrected) in both hemispheres.

Finally, we examined global brain connectivity differences between pFus-faces/FFA-1 and mFus-faces/FFA-2 by averaging RSFC values across 12 networks separately for each region to summarize these effects across networks. A 3-way between-subject ANOVA of the summarized RSFC with hemisphere (LH, RH), group (separate, continuous, single), and region (mFus-faces/FFA-2, pFus-faces/FFA-1) as factors (Fig. 4B, bar plot) revealed that across networks, pFus-faces/FFA-1 had a globally higher RSFC than mFus-faces/FFA-2 in the separate ($F(1, 3872)=202.81$, $p<.001$) and continuous group ($F(1, 3872)=56.49$, $p<.001$), but not the single group ($F(1, 3872)=.08$, $p=.780$).

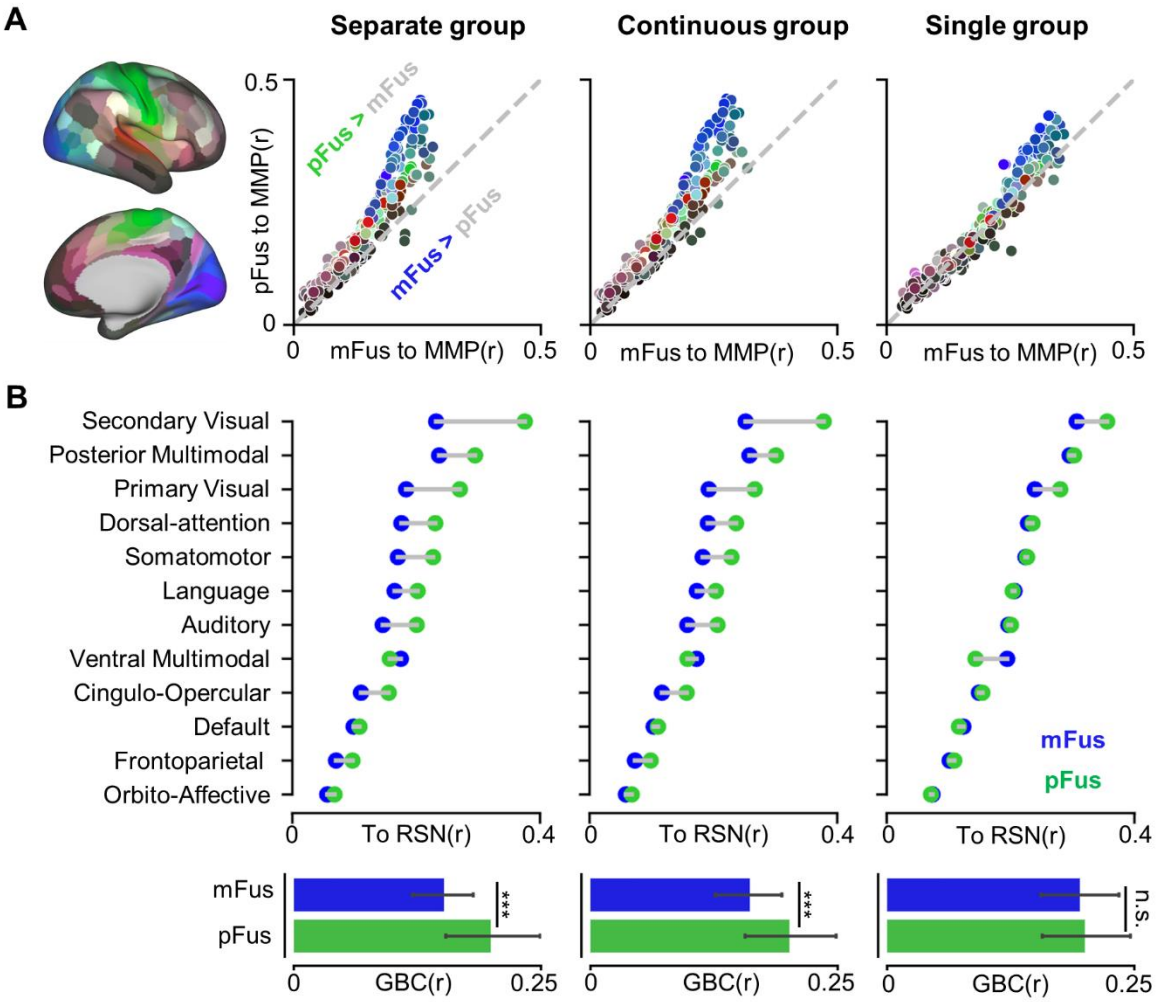

Figure 4. mFus-faces/FFA-2 and pFus-faces/FFA-1 have different resting-state functional connectivity (RSFC) "fingerprints". (A) pFus-faces/FFA-1 showed stronger RSFC than mFus-faces/FFA-2 to most of 358 HCP MMP areas in the separate and continuous groups. However, no difference between the two regions was observed in the single group. After averaging the two hemispheres, 179 areas were displayed as points on each scatter plot with color coding shown in the brain map at left. (B) pFus-faces/FFA-1 showed stronger RSFC than mFus-faces/FFA-2 to most of the 12 resting-state networks (RSNs) from (Ji et al., 2019) in the separate and continuous groups, and no difference between the two regions was found in the single group. Bar plots show global brain connectivity (GBC) for each face-selective region, calculated as mean RSFCs of each face-selective region across RSNs. Error bars indicate the 95% confidence interval; ***p<0.001; n.s., not significant; RSFCs displayed here were merged across hemispheres.

Spatial patterns of face selectivity and functional connectivity, but not anatomical features, in pFus-faces/FFA-1 and mFus-faces/FFA-2 were more similar between pairs of monozygotic than dizygotic twins

Are there heritable components contributing to the functional, structural, and connectivity differences between pFus-faces/FFA-1 and mFus-faces/FFA-2? Previous research indicates a genetic contribution to face processing ability (Wilmer et al., 2010; Wu et al., 2020; Zhu et al., 2010) and to the broad cortical morphology of category-selective regions in ventral temporal cortex (Abbasi et al., 2020). To test the above question that stems from these previous findings, we evaluated if spatial patterns of functional (face selectivity), connectivity (RSFC), macroanatomical (cortical thickness), and microstructural (myelination) features of pFus-faces/FFA-1 and mFus-faces/FFA-2 were more similar in monozygotic (MZ) than dizygotic (DZ) twins. We were able to do so because a subset of the 1080 participants within the HCP dataset are from 133 MZ pairs and 78 DZ pairs. The similarity of the spatial patterns from each twin pair was assessed by the Pearson correlation coefficient for each of the four functional or structural characteristics (Fig. 5). We found that the spatial patterns of face selectivity and functional connectivity, but not macroanatomical or microstructural features, of pFus-faces/FFA-1 and mFus-faces/FFA-2 were more similar between pairs of MZ than DZ twins. Specifically, significant main effects of zygosity were found for face selectivity ($F(1, 209)=37.60$, $p<.001$) and for RSFC ($F(1, 181)=42.71$, $p<.001$). Although there were interactions among zygosity, region, and hemisphere (Fs$(1, 181)>8.37$, ps$<.005$) for RSFC, the effects of zygosity within each level of hemisphere and region were significant (all Fs$(1, 181)>=13.04$, all ps$<.001$). Comparatively, there was no significant main effect of zygosity

for either cortical thickness ($F(1, 209)=1.50$, $p=.221$) or myelination ($F(1, 209)=3.39$, $p=.067$).

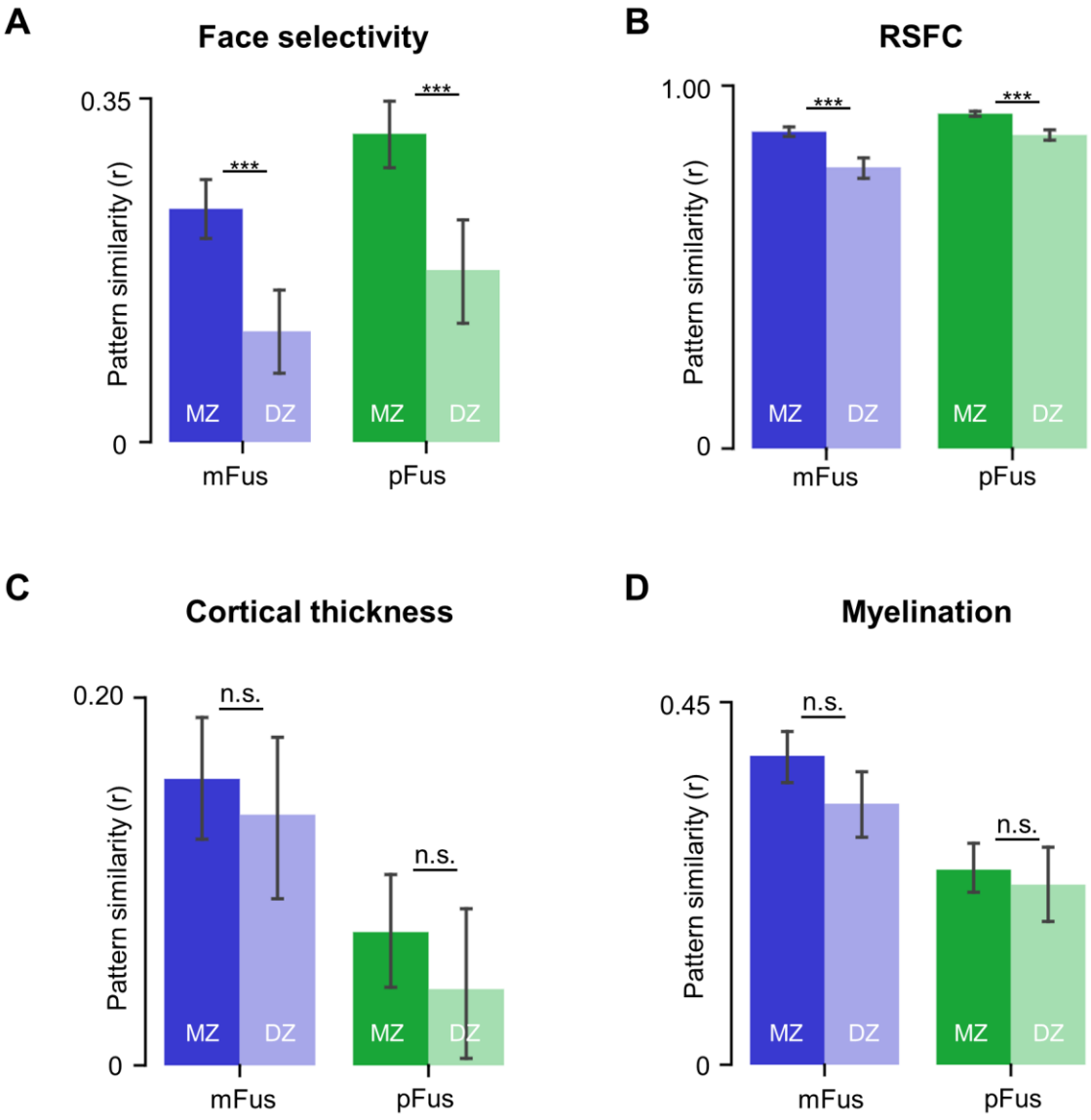

Figure 5. Spatial patterns of face selectivity and functional connectivity, but not anatomical features, in pFus-faces/FFA-1 and mFus-faces/FFA-2 were more similar between pairs of monozygotic (MZ) than dizygotic (DZ) twins. (A) MZ twins showed significantly higher spatial pattern similarity in face selectivity than DZ twins for both face-selective regions. (B) MZ twins showed significantly higher spatial pattern similarity in resting-state functional connectivity (RSFC) than DZ twins for both face-selective regions. (C) MZ twins and DZ twins showed no significant differences in spatial pattern similarity of cortical thickness within both face-selective regions. (D) MZ twins and DZ

373 twins showed no significant differences in spatial pattern similarity of myelination within both face-
374 selective regions. Error bars indicate the 95% confidence interval; ***p<0.001; n.s., not significant.
375

376 **DISCUSSION**

377

378 Parcellating the cerebral cortex into areas continues to be a major goal in
379 neuroscience. Over the last twenty-five years, the Fusiform Face Area (FFA) is one of the
380 most widely studied – and heavily debated – brain areas (Kanwisher, 2010, 2017;
381 Kanwisher et al., 1997). In addition to many theories proposed to explain how and why
382 humans and other mammals have neural responses selective for faces, researchers also
383 debate if the FFA is one contiguous area or not. However, these previous studies have
384 suffered from small sample sizes (often between 10 and 50 participants). Here, we
385 defined 4,221 face-selective regions on the fusiform gyrus (FG) in 1080 participants and
386 showed that 95.42% of hemispheres have not one, but two, face-selective regions on the
387 FG that are dissociable based on functional, macroanatomical, microstructural, and
388 connectivity features. Additionally, we showed that the spatial patterns of face selectivity
389 and functional connectivity are more highly correlated in monozygotic than dizygotic twins,
390 which was surprisingly not the case for anatomical features such as cortical thickness
391 and myelination. Below, we consider these results in the context of i) future studies
392 interested in the structure and function of face-selective regions on the FG, ii) individual
393 differences in anatomy, face selectivity, and face perception, iii) understanding the
394 complex relationship among genetics, anatomical gradients, and functional gradients, as
395 well as how that relationship relates to perception, and iv) group averages vs. individual
396 differences in neuroimaging studies.

397

Implications for future studies interested in the structure and function of face-selective regions on the FG

For more than a decade, dozens of studies have identified at least two face-selective regions on the FG (Çukur et al., 2013; Davidenko et al., 2012; Elbich & Scherf, 2017; Engell & McCarthy, 2013; Finzi et al., 2021; Gomez et al., 2015, 2017, 2018; Julian et al., 2012; Kay et al., 2015; Kietzmann et al., 2012; McGugin et al., 2014, 2015, 2016; Natu et al., 2016, 2019; Nordt et al., 2021; Parvizi et al., 2012; Pinsk et al., 2009; Rosenke et al., 2020, 2021; Scherf et al., 2017; Stigliani et al., 2015, 2019; Weiner et al., 2010, 2014, 2016, 2017; Weiner & Grill-Spector, 2010; Zhen et al., 2015) in addition to other face-selective regions in the core and extended systems of face processing (Haxby et al., 2000). Yet, to our knowledge, only two of these studies included more than 100 participants (N=121, Engell & McCarthy, 2013; N=202, Zhen et al., 2015) with the goal of generating probabilistic atlases. Critically, these two studies did not report individual differences in the structure or function of separate FG face-selective regions and the sample size was still a small percentage of that used in the present study. Here, we extend these previous studies by defining FG face-selective regions in over 1000 participants and show that the more posterior pFus-faces/FFA-1 is cortically thinner and more myelinated than the more anterior mFus-faces/FFA-2. Additionally, pFus-faces/FFA-1 is more face-selective with stronger functional connectivity to other cortical networks than mFus-faces/FFA-2.

Together, these results are surprising considering that it is widely accepted that identifying a single FFA is the norm, not the exception. Yet, our results empirically support the opposite in the largest group of manually defined face-selective regions on the FG to

421 date (to our knowledge). The present findings in combination with previous findings
422 showing cytoarchitectonic (Weiner et al., 2017) and functional differences between these
423 two regions (Kay et al., 2015; Weiner et al., 2010; Weiner & Grill-Spector, 2013), indicate
424 that our findings are not just a matter of splitting one FFA into two. Instead, a majority of
425 hemispheres contain two face-selective regions on the FG that are dissociable based on
426 functional, macroanatomical, microstructural, and connectivity features. Thus, a goal of
427 future empirical studies is to test for further functional differences between these regions,
428 as well as similarities and differences in their anatomical connectivity. Future theoretical
429 and computational work should also consider the FFA as two distinct regions in their
430 models, as well as a third region in the anterior FG that is often immeasurable with fMRI
431 due to methodological limitations (Jonas & Rossion, 2021). Finally, even though FG face-
432 selective regions are most often non-contiguous, the two regions together may constitute
433 a functionally distinct system separate from other face-selective regions as suggested
434 previously (Kanwisher, 2010) or perform the same function under certain task conditions
435 despite the structural and functional differences identified here (the idea of “degeneracy”;
436 Price and Friston, 2002; Edelman and Gally, 2001), both of which can be tested in future
437 studies.
438
439 *Genetics, anatomical gradients, and functional clusters on the human FG: Perceptual*
440 *consequences?*
441 Recent research indicates systematic relationships among gradients of genetic
442 expression (e.g. transcriptomics) relative to macroanatomical (e.g. cortical thickness),
443 and microstructural (e.g. myelination) cortical features (Burt et al., 2018; Gomez et al.,

2019). Additionally, recent findings also show that genetic expression in the brain is consistent with broad spatial trends that align well with network and connectomic architecture (Fornito et al., 2020), as well as functional maps within cortical areas (Gomez et al., 2021). The present results add additional novel insights to these previous findings. For example, even though there is a relationship among transcriptomics, cortical thickness, and myelination in the FG and more broadly across the visual processing hierarchy in humans (Gomez et al., 2019), there is a stronger correlation in MZ than DZ twins for face selectivity and connectivity properties of FG face-selective regions, but not cortical thickness and myelination. The latter finding indicates the utility of using different types of complementary data to improve our understanding of the complex relationship among genetics, anatomical gradients, and functional representations (gradients, maps, and clusters) in the human brain. As previous research shows genetic contributions also to face perception (Wilmer et al., 2010; Zhu et al., 2010) and the neural processing of faces (Abbasi et al., 2020; Brown et al., 2012), future studies can examine genetic contributions relating the structural and functional features of these FG face-selective regions to face processing ability.

For instance, does genetic expression contribute to the number of face-selective regions on the FG, which in turn, contributes to face processing ability? More broadly, what are the behavioral implications for only having one of these face-selective regions on the FG – or none at all? For example, there is recent causal evidence showing that electrical brain stimulation (EBS) to mFus-faces/FFA-2 results in deficits in naming faces, while EBS to pFus-faces/FFA-1 results in face-specific perceptual distortions (Schrouff et al., 2020). Such a result suggests that only having either mFus-faces/FFA-2 or pFus-

faces/FFA-1 could have an effect on neural representations of either faces themselves in pFus-faces/FFA-1 or the integration of information about person identity in mFus-faces/FFA-2, which can be further examined in future studies. Additional recent findings also suggest that anatomical and morphological features of each region is related to face perception. For example, McGugin and colleagues (2016) showed that cortical thickness of pFus-faces/FFA-1 contributed more to behavioral performance on a face processing task than did mFus-faces/FFA-2 (McGugin et al., 2016). Additionally, the size of pFus-faces/FFA-1 was more tightly linked to behavior on a face processing task than the size of mFus-faces/FFA-2 (Elbich & Scherf, 2017). The combination of these causal and correlational results are consistent with the present results showing that pFus-faces/FFA-1 is more face-selective than mFus-faces/FFA-2. Taken together, the present findings lay the foundation for future work and mechanistic models linking genetics to face processing relative to underlying functional, structural, and connectivity differences between mFus-faces/FFA-2 and pFus-faces/FFA-1.

Averages vs. individual differences in neuroimaging studies

A continued debate in the broader neuroimaging field is the balance between averages and group analyses compared to individual differences and analyses at the level of individual participants (Coalson et al., 2018; Friston et al., 2006; Poldrack et al., 2015; Saxe et al., 2006; Van Essen & Glasser, 2018). Directly related to this debate and the present findings, Van Essen and Glasser (2018) qualitatively showed that a group definition of the FFA (or what they referred to as a “strip-like” fusiform face complex, FFC) defined using the same dataset as used here does not align well with individual

differences in the definition of face-selective regions on the FG in individual hemispheres. This observation is consistent with the present results showing that a majority of participants have two cortically distinct face-selective regions on the mid and posterior FG and even when there is one "strip-like" activation, it can be subdivided into two components that are functionally, macroanatomically, and microstructurally distinct from one another with different functional connectivity profiles.

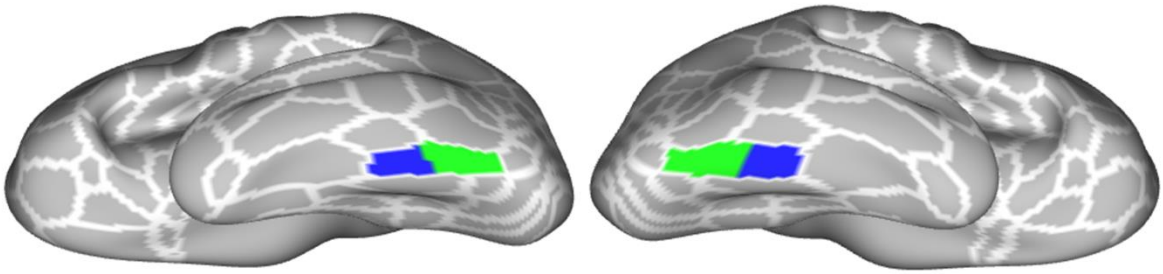

Figure 6. Multimodal parcellation of area FFC. Inflated cortical surface reconstructions of the left and right hemisphere in 32k_fs_LR space. White lines are outlines of areas in the HCP MMP Atlas. Green and blue shaded areas indicate multimodal parcellations of area FFC into mFus-faces/FFA-2 (blue) and pFus-faces/FFA-1 (green), which to our knowledge, is the first empirical modification of an area within the recently proposed multimodal map of the human cerebral cortex (Glasser et al., 2016), as well as the first conducted at the level of individual participants.

Moving forward, then, how do we i) strike a balance between group averages and individual differences (when both are necessary and complement one another) and ii) overcome the fact that defining regions of interest (ROIs) manually is monotonous, requires expertise, typically limits sample sizes, and limits the cortical expanse a particular study can explore? Here, we propose that a deep learning approach implemented previously on just the cortical anatomy, could also be implemented on functional definitions to improve the accuracy of automated definitions of functional brain regions in individual participants. Specifically, two recent studies (Borne et al., 2020; Lyu

et al., 2021) used deep learning approaches to define sulci in individual participants with significant success. Each study first used many trained raters to manually define thousands of sulci and then trained and tested deep learning algorithms to label each sulcus. The algorithms accurately defined all sulci, but were the most accurate for deeper sulci that often had larger surface areas. This would suggest that once functional regions are manually defined in individual participants, the same algorithms could be trained, tested, and used to define functional regions in new participants. As the algorithms often improve as more data are used for training, functional ROIs defined in large, freely available datasets such as the multimodal data of the HCP at 3T and the retinotopy data of the HCP at 7T are good starting points for future studies to test the feasibility of this proposal. If successful, this approach would allow relatively automated approaches for accurate definitions of functional regions in individual participants – we use “relatively” here because the algorithms will first need to be trained on manually defined functional regions. In the interim, as we share our definitions with the field (Fig. 6), future studies can perform novel multimodal analyses that leverage the rich multimodal HCP dataset to explore how anatomical and functional features of these face-selective regions relate to cognitive and behavioral metrics also acquired in each participant without needing the expertise to define each region manually. Finally, this approach also does not solve the balance between group analyses and analyses in individual participants for tasks, behaviors, and cognitive phenemona for which cortical regions and networks remain unknown.

CONCLUSION

In sum, we examined individual differences of fusiform face area(s) in a large group (N>1000) of participants for the first time. Our results show that identifying a single FFA is actually the exception, not the norm as described in the broader literature. Instead, it is most common to identify two face-selective regions on the lateral FG that are 2.27 cm apart on average between the most face-selective vertices, as well as are dissociable based on functional, macroanatomical, microstructural, and connectivity features. This organization of clustered regions or patches as opposed to a single larger area aligns well with face-selective patches identified in other species, such as macaques. Additionally, functional (face selectivity) and connectivity (RSFC) features are more highly correlated in monozygotic compared to dizygotic twins, while structural features (cortical thickness, myelination) are not. Future studies can leverage the fact that we are sharing our 4,221 manual areal definitions with the field (http://www.brainactivityatlas.org/atlas/atlas-download; Fig. 6) to further explore how functional, structural, and connectivity features of these regions relate to cognitive and behavioral metrics also acquired in each participant within the rich multimodal HCP dataset.

MATERIALS AND METHODS

Data overview

HCP-Young Adult (HCP-YA, S1200 data release, 2017) data were used to define two face-selective regions on the fusiform gyrus (pFus-faces/FFA-1, mFus-faces/FFA-2) and to compare their i) macrostructure (cortical thickness), ii) microstructure (myelination), iii) face selectivity, and iv) resting-state functional connectivity (RSFC) profiles. Additionally, spatial patterns of these structural and functional features were compared between each region in pairs of monozygotic and dizygotic twins. The HCP-YA includes behavioral and multi-modal MRI data from 1206 healthy young adult participants (i.e., S1200). After excluding the subjects with incomplete MRI scans, 1080 participants (586 females, ages 22 to 37) were retained, each of whom completed structural MRI (sMRI), resting-state functional MRI (rfMRI), and task functional MRI (tfMRI) scans (Van Essen et al., 2013). Among them, there are 211 twin pairs (133 monozygotic (MZ) twins and 78 dizygotic (DZ) twins, M/F: 172/250). All participants provided written informed consent. MRI protocols were approved by the Institutional Review Board (IRB) of Washington University.

MRI acquisition

The HCP-YA MRI data were acquired on the HCP's custom 3T Siemens Skyra scanner using a 32-channel head coil. T1-weighted (T1w) images were acquired using the 3D MPRAGE sequence (TR = 2400 ms, TE = 2.14 ms, voxel size = 0.7 mm isotropic, iPAT = 2). T2-weighted (T2w) images were acquired using the 3D SPACE sequence (TR = 3200 ms, TE = 565 ms, voxel size = 0.7 mm isotropic, iPAT = 2). Functional data were

576 acquired using gradient-echo EPI sequence (TR = 720 ms, TE = 33.1 ms, voxel size = 2
577 mm isotropic, MB = 8). Four runs of rfMRI data were acquired for each participant from
578 the HCP-YA, each of which were approximately 15 minutes. Details of the HCP-YA MRI
579 acquisition can be found elsewhere (Barch et al., 2013; Glasser et al., 2013; Smith et al.,
580 2013; Uğurbil et al., 2013).
581
582 *Functional localizer*
583 Face-selective regions were localized using a working memory task in which four
584 stimulus types (faces, places, tools, and body parts) were presented in separate blocks
585 (Barch et al., 2013). The localizer consisted of two runs, and each run contained eight
586 task blocks (10 trials of 2.5 s each, for 25 s) and 4 fixation blocks (15 s each). Within each
587 run, half of the task blocks used a 2-back working memory task and the other half
588 implemented a 0-back working memory task. A 2.5 s cue indicated the task type at the
589 start of the block. For each trial, the stimulus was presented for 2 s, followed by a 500 ms
590 inter-trial interval (ITI).
591
592 *Emotion processing paradigm*
593 In each of two runs, participants were presented with 3 face blocks and 3 shape
594 blocks (21 s each) (Barch et al., 2013). Each block, preceded by a 3 s task cue ("shape"
595 or "face"), had 6 trials (2 s each, with a 1 s ITI). When the stimulus was presented,
596 participants decided which of two faces/shapes presented on the bottom of the screen
597 matched the face/shape at the top of the screen. The faces had either angry or fearful
598 expressions.

MRI preprocessing

The MRI data of HCP-YA were preprocessed with the HCP minimal preprocessing pipelines (Glasser et al., 2013). The T1w and T2w images were used to i) reconstruct individual cortical surfaces, ii) estimate the T1w/T2w ratio (which is a measure of tissue contrast enhancement that is a proxy for myelination), and iii) cortical thickness. The individual surfaces and related maps were further registered to the standard fsLR surface via the multimodal surface matching (MSM) algorithm (Glasser et al., 2016; Robinson et al., 2014). All functional images from individual participants were motion corrected, temporally filtered (highpass filter, cutoff = 2000 s), spatially denoised via the ICA+FIX approach, and registered to the standard CIFTI grayordinate fsLR space using the MSM algorithm. The preprocessed task fMRI data were entered into a general linear model (GLM) to estimate fMRI activity at each vertex/voxel in each run with FSL (FMRIB's Software Library, www.fmrib.ox.ac.uk/fsl) (Barch et al., 2013). The boxcar convolved with a double gamma hemodynamic response function, and its temporal derivative was used to model the BOLD responses. Linear contrasts were computed to estimate effects of interest (e.g., faces vs. others; faces vs. shapes). Fixed-effects analyses were conducted to estimate the average effects across runs within each participant. No spatial smoothing was implemented.

Manual definition of mFus-faces/FFA-2 and pFus-faces/FFA-1 in over 1,000 participants

Face-selective regions on the lateral fusiform gyrus (FG) were manually delineated for each hemisphere and each participant based on individual, thresholded (Z>1.65,

622 p<0.05, uncorrected) face-selective activation maps (faces versus others). From this
623 thresholded map, face-selective regions were labeled as either mFus-faces/FFA-2 or
624 pFus-faces/FFA-1 based on previously published criteria differentiating the cortical
625 location of the two regions relative to sulci within and surrounding the FG (Fig. 1A).
626 Specifically, mFus-faces/FFA-2 is coupled with the anterior tip of the mid-fusiform sulcus
627 (MFS) whereas pFus-faces/FFA-1 is located on the posterior aspect of the FG, extending
628 into the occipito-temporal sulcus (Weiner, 2019; Weiner et al., 2014). To define each
629 region, we implemented a three-pronged approach. First, author X.C. labeled each region
630 manually on the individual thresholded face-selective map with a customized software
631 (FreeROI, https://github.com/BNUCNL/FreeROI). Second, author Z.Z. checked the
632 regions and refined them together with X.C. Third, author K.S.W. finalized the regions.
633
634 *Incidence rates and surface area of mFus-faces/FFA-2 and pFus-faces/FFA-1*
635 Overall, we categorized the spatial organization of mFus-faces/FFA-2 and pFus-
636 faces/FFA-1 into three types, or topological groups, (Fig. 1B): separate, continuous, and
637 single. The “separate” group consisted of two cortically distinct face-selective regions in
638 a given hemisphere that were separated by a cortical gap. The “continuous” group
639 consisted of two regions that were identifiable and contiguous, but could be separated
640 based on previously proposed anatomical criteria based on cortical folding (Weiner, 2019;
641 Weiner et al., 2014). The “single” group consisted of one region in which either mFus-
642 faces/FFA-2 or pFus-faces/FFA-1, but not both, was identifiable in a given hemisphere.
643 After determining these three groups, we summarized the incidence rate of each group
644 by counting how many hemispheres were in each group. The surface area of each region

was also quantified. A 3-way between-subject ANOVA with hemisphere (LH, RH), group (single, continuous, separate), and region (pFus-faces/FFA-1, mFus-faces/FFA-2) as factors was conducted to test the differences of surface area of each region among the three groups.

Cortical distance between pFus-faces/FFA-1 and mFus-faces/FFA-2

Geodesic distance was used to quantify the cortical distance between pFus-faces/FFA-1 and mFus-faces/FFA-2 by using the tvb-gdist package (https://github.com/the-virtual-brain/tvb-gdist). Geodesic distance is the length of the shortest line between two vertices on a triangulated mesh in three dimensions, such that the line lies on the surface. The cortical distance between the most face-selective vertices (i.e., the activation peaks) of the two regions was calculated for hemispheres from continuous and separate groups and a 2-way between-subject ANOVA was conducted to test the effects of hemisphere (LH, RH) and group (continuous, separate) on the distance. In addition, the cortical gap between two regions was measured for the separate group by calculating the minimum geodesic distance between the vertices of the two regions, and a two-sample t-test was performed to test the interhemispheric differences of the gaps.

The spatial consistency of mFus-faces/FFA-2 and pFus-faces/FFA-1 across groups

A group-specific probabilistic map was created for each fusiform face-selective region in each group (separate, continuous, single) to characterize the likelihood that a given vertex belongs to that region across the participants on whom either pFus-

faces/FFA-1, mFus-faces/FFA-2, or both had been identified. For each region, the spatial consistency was calculated as the spatial pattern similarity between each pair of group-specific probabilistic maps. Specifically, the spatial patterns in the overlapped portion of each pair of group probabilistic maps were extracted to compute the Pearson correlation coefficient.

Average cortical thickness and myelination of pFus-faces/FFA-1 and mFus-faces/FFA-2

We tested if pFus-faces/FFA-1 and mFus-faces/FFA-2 were anatomically distinct by calculating average macroanatomical (e.g., cortical thickness) and microstructural (e.g., myelination) values from each region in each individual. The mean thickness and myelination values were generated by averaging each measurement across all vertices within each region in each hemisphere and participant within each of the three groups. A 4-way between-subject ANOVA with metric (myelination, thickness), hemisphere (LH, RH), group (single, contiguous, separate), and region (pFus-faces/FFA-1, mFus-faces/FFA-2) as factors was then conducted to test significant main effects and interactions of these factors. In addition, a separate 3-way between-subject ANOVA was conducted to further examine the effects of hemisphere (LH, RH), group (single, contiguous, separate), and region (pFus-faces/FFA-1, mFus-faces/FFA-2) on myelination content.

Comparing face-selectivity between mFus-faces/FFA-2 and pFus-faces/FFA-1

As pFus-faces/FFA-1 and mFus-faces/FFA-2 are defined based on the HCP working memory task, we used face and shape conditions from the emotional processing

task, which was also included in the HCP dataset, as an additional independent dataset to compare face selectivity between the two face-selective regions in each of the three groups. These data were acquired in nearly all participants (939/1080 participants) and were completely independent from the data used to define each face-selective region. Face selectivity was quantified as the average z-value of the contrast (faces vs. shapes) within each functional region in each individual participant. A 3-way between-subject ANOVA with hemisphere (LH, RH), group (single, continuous, separate), and region (pFus-faces/FFA-1, mFus-faces/FFA-2) as factors was conducted to test if pFus-faces/FFA-1 or mFus-faces/FFA-2 differed in their mean face-selectivity.

Comparing resting state functional connectivity profiles between mFus-faces/FFA-2 and pFus-faces/FFA-1

To quantify network connectivity differences between these two face-selective regions, we considered three scales i) areal, ii) network, and iii) global. At the areal level, we quantified the resting-state functional connectivity (RSFC) from each FG face-selective region to each of the HCP MMP areas (Glasser et al., 2016) except the FFC (which includes mFus-faces/FFA-2 and pFus-faces/FFA-1). In detail, for each participant, RSFCs between each face-selective region and each of HCP MMP cortical areas were derived for each run by calculating Pearson correlation coefficients between their resting-state BOLD time courses, and then averaged across the four runs. At the network level, we characterized the connectivity of the two face-selective regions to the twelve large-scale resting-state networks (RSNs) by summarizing the RSFCs to all MMP areas into 12-dimension RSFC “fingerprints” according to Cole-Anticevic Brain Network Parcellation

(CAB-NP) (Ji et al., 2019). At the global level, we characterized the global brain connectivity (Cole et al., 2010) of each face-selective region by averaging RSFC values across the twelve large-scale networks. At both areal and network levels, two-sample t-tests were conducted to compare RSFCs of pFus-faces/FFA-1 and mFus-faces/FFA-2, and false discovery rate (FDR) corrections were conducted for the 358/12 tests in each hemisphere and each group, respectively. At the global brain level, a 3-way between-subject ANOVA with hemisphere (LH, RH), group (single, continuous, separate), and region (pFus-faces/FFA-1, mFus-faces/FFA-2) as factors was conducted to test the inter-regional differences in connectivity.

Comparing spatial patterns of functional, structural, and connectivity features of pFus-faces/FFA-1 and mFus-faces/FFA-2 between pairs of monozygotic and dizygotic twins

Are there heritable components contributing to the functional, connectivity, macroanatomical, and microstructural differences between pFus-faces/FFA-1 and mFus-faces/FFA-2? To test this question, we evaluated if spatial patterns of functional (face selectivity), connectivity (RSFC), macroanatomical (cortical thickness), and microstructural (myelination) features of pFus-faces/FFA-1 or mFus-faces/FFA-2 were more similar in monozygotic (MZ) than dizygotic (DZ) twins. We were able to do so because a subset of the 1080 participants within the HCP dataset are from 133 MZ pairs and 78 DZ pairs. Since individual ROIs are different and we cannot quantitatively compare ROI matrices that are unequal in size, the maximum probability map (MPM) of mFus-faces/FFA-2 and pFus-faces/FFA-1 were used for these analyses. Specifically, the spatial patterns of face selectivity, thickness, and myelination of pFus-faces/FFA-1 and mFus-

737 faces/FFA-2 were directly extracted from the MPM masks and the spatial pattern of RSFC
738 of each face-selective region was characterized as the RSFC fingerprint between its MPM
739 mask and the 12 RSNs. The similarity of the spatial patterns from each twin pair was
740 assessed by the Pearson correlation coefficient, and a 2 (zygosity: MZ, DZ; between-
741 subject) × 2 (region: pFus-faces/FFA-1, mFus-faces/FFA-2; within-subject) × 2
742 (hemisphere: left, right; within-subject) ANOVA was conducted to statistically compare
743 similarities in each anatomical (thickness, myelination) and functional (face selectivity,
744 functional connectivity) feature.
745

746 **REFERENCES**

747

748 Abbasi, N., Duncan, J., & Rajimehr, R. (2020). Genetic influence is linked to cortical
749 morphology in category-selective areas of visual cortex. *Nature Communications*,
750 *11*(1), 709. https://doi.org/10.1038/s41467-020-14610-8
751 Apurva, N., Murty, R., Teng, S., Beeler, D., Mynick, A., Oliva, A., Kanwisher, N.,
752 Leopold, D. A., & Op De Beeck, H. (2004). Visual experience is not necessary for
753 the development of face-selectivity in the lateral fusiform gyrus. *PNAS*, *117*(37),
754 23011–23020. https://doi.org/10.1073/pnas.2004607117
755 Arcaro, M. J., Schade, P. F., & Livingstone, M. S. (2019). Universal mechanisms and
756 the development of the face network: What you see Is What You Get. In *Annual*
757 *Review of Vision Science* (Vol. 5, pp. 341–372). https://doi.org/10.1146/annurev-
758 vision-091718-014917
759 Avidan, G., & Behrmann, M. (2021). Spatial integration in normal face processing and
760 its breakdown in congenital prosopagnosia. *Annual Review of Vision Science*, *7*,
761 301–321. https://doi.org/10.1146/annurev-vision-113020-012740
762 Barch, D. M., Burgess, G. C., Harms, M. P., Petersen, S. E., Schlaggar, B. L., Corbetta,
763 M., Glasser, M. F., Curtiss, S., Dixit, S., Feldt, C., Nolan, D., Bryant, E., Hartley,
764 T., Footer, O., Bjork, J. M., Poldrack, R., Smith, S., Johansen-Berg, H., Snyder,
765 A. Z., … WU-Minn HCP Consortium. (2013). Function in the human connectome:
766 Task-fMRI and individual differences in behavior. *NeuroImage*, *80*, 169–189.
767 https://doi.org/10.1016/j.neuroimage.2013.05.033
768 Behrmann, M., & Plaut, D. C. (2013). Distributed circuits, not circumscribed centers,
769 mediate visual recognition. *Trends Cogn Sci*, *17*(5), 210–219.
770 https://doi.org/10.1016/j.tics.2013.03.007
771 Bell, A. H., Malecek, N. J., Morin, E. L., Hadj-Bouziane, F., Tootell, R. B., & Ungerleider,
772 L. G. (2011). Relationship between functional magnetic resonance imaging-
773 identified regions and neuronal category selectivity. *J Neurosci*, *31*(34), 12229–
774 12240. https://doi.org/10.1523/jneurosci.5865-10.2011
775 Benson, N. C., Yoon, J. M. D., Forenzo, D., Kay, K. N., Engel, S. A., & Winawer, J.
776 (2021). Variability of the surface area of the V1, V2, and V3 maps in a large

777 sample of human observers. *BioRxiv*, 2020.12.30.424856.
778 https://doi.org/10.1101/2020.12.30.424856
779 Borne, L., Rivière, D., Mancip, M., & Mangin, J.-F. (2020). Automatic labeling of cortical
780 sulci using patch- or CNN-based segmentation techniques combined with
781 bottom-up geometric constraints. *Medical Image Analysis*, *62*, 101651.
782 https://doi.org/10.1016/j.media.2020.101651
783 Brown, A. A., Jensen, J., Nikolova, Y. S., Djurovic, S., Agartz, I., Server, A., Ferrell, R.
784 E., Manuck, S. B., Mattingsdal, M., Melle, I., Hariri, A. R., Frigessi, A., &
785 Andreassen, O. A. (2012). Genetic variants affecting the neural processing of
786 human facial expressions: Evidence using a genome-wide functional imaging
787 approach. *Translational Psychiatry*, *2*, e143. https://doi.org/10.1038/tp.2012.67
788 Burt, J. B., Demirtaş, M., Eckner, W. J., Navejar, N. M., Ji, J. L., Martin, W. J.,
789 Bernacchia, A., Anticevic, A., & Murray, J. D. (2018). Hierarchy of transcriptomic
790 specialization across human cortex captured by structural neuroimaging
791 topography. *Nature Neuroscience*, *21*(9), 1251–1259.
792 https://doi.org/10.1038/s41593-018-0195-0
793 Coalson, T. S., Essen, D. C. V., & Glasser, M. F. (2018). The impact of traditional
794 neuroimaging methods on the spatial localization of cortical areas. *Proceedings*
795 *of the National Academy of Sciences*, *115*(27), E6356–E6365.
796 https://doi.org/10.1073/pnas.1801582115
797 Cohen, M. A., Dilks, D. D., Koldewyn, K., Weigelt, S., Feather, J., Kell, A. J., Keil, B.,
798 Fischl, B., Zöllei, L., Wald, L., Saxe, R., & Kanwisher, N. (2019).
799 Representational similarity precedes category selectivity in the developing ventral
800 visual pathway. *NeuroImage*, *197*, 565–574.
801 https://doi.org/10.1016/j.neuroimage.2019.05.010
802 Cole, M. W., Pathak, S., & Schneider, W. (2010). Identifying the brain's most globally
803 connected regions. *NeuroImage*, *49*(4), 3132–3148.
804 https://doi.org/10.1016/j.neuroimage.2009.11.001
805 Çukur, T., Huth, A. G., Nishimoto, S., & Gallant, J. L. (2013). Functional subdomains
806 within human FFA. *Journal of Neuroscience*, *33*(42), 16748–16766.
807 https://doi.org/10.1523/JNEUROSCI.1259-13.2013

Davidenko, N., Remus, D. A., & Grill-Spector, K. (2012). Face-likeness and image variability drive responses in human face-selective ventral regions. *Human Brain Mapping*, *33*(10), 2334–2349. https://doi.org/10.1002/hbm.21367

Deen, B., Richardson, H., Dilks, D. D., Takahashi, A., Keil, B., Wald, L. L., Kanwisher, N., & Saxe, R. (2017). Organization of high-level visual cortex in human infants. *Nature Communications*, *8*(1), 13995. https://doi.org/10.1038/ncomms13995

Downing, P. E., Chan, A. W.-Y., Peelen, M. V., Dodds, C. M., & Kanwisher, N. (2006). Domain specificity in visual cortex. *Cerebral Cortex*, *16*(10), 1453–1461. https://doi.org/10.1093/cercor/bhj086

Duchaine, B., & Yovel, G. (2015). A revised neural framework for face processing. *Annual Review of Vision Science*, *1*(1), 393–416. https://doi.org/10.1146/annurev-vision-082114-035518

Edelman, G. M., & Gally, J.A. (2001). Degeneracy and complexity in biological systems. *Proceedings of the National Academy of Sciences of the United States of America*, *98*(24), 13763-13768. https://doi.org/10.1073/pnas.231499798

Elbich, D. B., & Scherf, S. (2017). Beyond the FFA: Brain-behavior correspondences in face recognition abilities. *NeuroImage*, *147*, 409–422. https://doi.org/10.1016/j.neuroimage.2016.12.042

Engell, A. D., & McCarthy, G. (2013). Probabilistic atlases for face and biological motion perception: An analysis of their reliability and overlap. *NeuroImage*, *74*, 140–151. https://doi.org/10.1016/j.neuroimage.2013.02.025

Finzi, D., Gomez, J., Nordt, M., Rezai, A. A., Poltoratski, S., & Grill-Spector, K. (2021). Differential spatial computations in ventral and lateral face-selective regions are scaffolded by structural connections. *Nature Communications*, *12*(1), 2278. https://doi.org/10.1038/s41467-021-22524-2

Fornito, A., Arnatkeviciute, A., Fulcher, B., Oldham, S., Tiego, J., & Bellgrove, M. (2020). Genetic influences on brain network hubs. *Biological Psychiatry*, *87*(9, Supplement), S86–S87. https://doi.org/10.1016/j.biopsych.2020.02.243

Friston, K. J., Rotshtein, P., Geng, J. J., Sterzer, P., & Henson, R. N. (2006). A critique of functional localisers. *NeuroImage*, *30*(4), 1077–1087. https://doi.org/10.1016/j.neuroimage.2005.08.012

839 Gauthier, I., Skudlarski, P., Gore, J. C., & Anderson, A. W. (2000). Expertise for cars
840 and birds recruits brain areas involved in face recognition. *Nat Neurosci*, *3*(2),
841 191–197. https://doi.org/10.1038/72140
842 Gauthier, I., Tarr, M. J., Anderson, A. W., Skudlarski, P., & Gore, J. C. (1999). Activation
843 of the middle fusiform "face area" increases with expertise in recognizing novel
844 objects. *Nat Neurosci*, *2*(6), 568–573. https://doi.org/10.1038/9224
845 Glasser, M. F., Coalson, T. S., Robinson, E. C., Hacker, C. D., Harwell, J., Yacoub, E.,
846 Ugurbil, K., Andersson, J., Beckmann, C. F., Jenkinson, M., Smith, S. M., & Van
847 Essen, D. C. (2016). A multi-modal parcellation of human cerebral cortex.
848 *Nature*, *536*(7615), 171–178. https://doi.org/10.1038/nature18933
849 Glasser, M. F., Sotiropoulos, S. N., Wilson, J. A., Coalson, T. S., Fischl, B., Andersson,
850 J. L., Xu, J., Jbabdi, S., Webster, M., Polimeni, J. R., Van Essen, D. C.,
851 Jenkinson, M., & WU-Minn HCP Consortium. (2013). The minimal preprocessing
852 pipelines for the Human Connectome Project. *NeuroImage*, *80*, 105–124.
853 https://doi.org/10.1016/j.neuroimage.2013.04.127
854 Golarai, G., Ghahremani, D. G., Whitfield-Gabrieli, S., Reiss, A., Eberhardt, J. L.,
855 Gabrieli, J. D. E., & Grill-Spector, K. (2007). Differential development of high-
856 level visual cortex correlates with category-specific recognition memory. *Nature*
857 *Neuroscience*, *10*(4), 512–522. https://doi.org/10.1038/nn1865
858 Golarai, G., Hong, S., Haas, B. W., Galaburda, A. M., Mills, D. L., Bellugi, U., Grill-
859 Spector, K., & Reiss, A. L. (2010). The fusiform face area is enlarged in Williams
860 syndrome. *The Journal of Neuroscience: The Official Journal of the Society for*
861 *Neuroscience*, *30*(19), 6700–6712. https://doi.org/10.1523/JNEUROSCI.4268-
862 09.2010
863 Gomez, J., Barnett, M. A., Natu, V., Mezer, A., Palomero-Gallagher, N., Weiner, K. S.,
864 Amunts, K., Zilles, K., & Grill-Spector, K. (2017). Microstructural proliferation in
865 human cortex is coupled with the development of face processing. *Science*,
866 *355*(6320), 68–71. https://doi.org/10.1126/science.aag0311
867 Gomez, J., Natu, V., Jeska, B., Barnett, M., & Grill-Spector, K. (2018). Development
868 differentially sculpts receptive fields across early and high-level human visual

cortex. *Nature Communications*, *9*(1), 788. https://doi.org/10.1038/s41467-018-03166-3

Gomez, J., Pestilli, F., Witthoft, N., Golarai, G., Liberman, A., Poltoratski, S., Yoon, J., & Grill-Spector, K. (2015). Functionally defined white matter reveals segregated pathways in human ventral temporal cortex associated with category-specific processing. *Neuron*, *85*(1), 216–227. https://doi.org/10.1016/j.neuron.2014.12.027

Gomez, J., Zhen, Z., & Weiner, K. S. (2019). Human visual cortex is organized along two genetically opposed hierarchical gradients with unique developmental and evolutionary origins. *PLOS Biology*, *17*(7), e3000362. https://doi.org/10.1371/journal.pbio.3000362

Gomez, J., Zhen, Z., & Weiner, K. S. (2021). The relationship between transcription and eccentricity in human V1. *Brain Structure and Function*, *226,* 2807–2818.

Grill-Spector, K., Golarai, G., & Gabrieli, J. (2008). Developmental neuroimaging of the human ventral visual cortex. *Trends in Cognitive Sciences*, *12*(4), 152–162. https://doi.org/10.1016/j.tics.2008.01.009

Grill-Spector, K., Knouf, N., & Kanwisher, N. (2004). The fusiform face area subserves face perception, not generic within-category identification. *Nature Neuroscience*, *7*(5), 555–562. https://doi.org/10.1038/nn1224

Grill-Spector, K., & Weiner, K. S. (2014). The functional architecture of the ventral temporal cortex and its role in categorization. *Nat Rev Neurosci*, *15*(8), 536–548. https://doi.org/10.1038/nrn3747

Grill-Spector, K., Weiner, K. S., Kay, K., & Gomez, J. (2017). The functional neuroanatomy of human face perception. *Annual Review of Vision Science*, *3*, 167-196. https://doi.org/10.1146/annurev-vision-102016-061214

Haxby, J. V, Gobbini, M. I., Furey, M. L., Ishai, A., Schouten, J. L., & Pietrini, P. (2001). Distributed and overlapping representations of faces and objects in ventral temporal cortex. *Science*, *293*(5539), 2425–2430. https://doi.org/10.1126/science.1063736

Haxby, J. V, Guntupalli, J. S., Connolly, A. C., Halchenko, Y. O., Conroy, B. R., Gobbini, M. I., Hanke, M., & Ramadge, P. J. (2011). A common, high-dimensional model

of the representational space in human ventral temporal cortex. *Neuron*, *72*(2), 404–416. https://doi.org/10.1016/j.neuron.2011.08.026

Haxby, J. V, Hoffman, E. A., & Gobbini, M. I. (2000). The distributed human neural system for face perception. *Trends Cogn Sci*, *4*(6), 223–233. https://doi.org/10.1016/s1364-6613(00)01482-0

Huth, A. G., De Heer, W. A., Griffiths, T. L., Theunissen, F. E., & Gallant, J. L. (2016). Natural speech reveals the semantic maps that tile human cerebral cortex. *Nature*, *532*(7600), 453–458. https://doi.org/10.1038/nature17637

Huth, A. G., Nishimoto, S., Vu, A. T., & Gallant, J. L. (2012). A continuous semantic space describes the representation of thousands of object and action categories across the human brain. *Neuron*, *76*(6), 1210–1224. https://doi.org/10.1016/j.neuron.2012.10.014

Ji, J. L., Spronk, M., Kulkarni, K., Repovš, G., Anticevic, A., & Cole, M. W. (2019). Mapping the human brain's cortical-subcortical functional network organization. *NeuroImage*, *185*, 35–57. https://doi.org/10.1016/j.neuroimage.2018.10.006

Jonas, J., Brissart, H., Hossu, G., Colnat-Coulbois, S., Vignal, J.-P., Rossion, B., & Maillard, L. (2018). A face identity hallucination (palinopsia) generated by intracerebral stimulation of the face-selective right lateral fusiform cortex. *Cortex; a Journal Devoted to the Study of the Nervous System and Behavior*, *99*, 296–310. https://doi.org/10.1016/j.cortex.2017.11.022

Jonas, J., & Rossion, B. (2021). Intracerebral electrical stimulation to understand the neural basis of human face identity recognition. *The European Journal of Neuroscience, 54*(1), 4197-4211. https://doi.org/10.1111/ejn.15235

Julian, J. B., Fedorenko, E., Webster, J., & Kanwisher, N. (2012). An algorithmic method for functionally defining regions of interest in the ventral visual pathway. *NeuroImage*, *60*(4), 2357–2364. https://doi.org/10.1016/j.neuroimage.2012.02.055

Kanwisher, N. (2000). Domain specificity in face perception. *Nat Neurosci*, *3*(8), 759–763. https://doi.org/10.1038/77664

Kanwisher, N. (2010). Functional specificity in the human brain: A window into the functional architecture of the mind. *Proceedings of the National Academy of*

Sciences of the United States of America, *107*(25), 11163–11170. https://doi.org/10.1073/pnas.1005062107

Kanwisher, N. (2017). The quest for the FFA and where It led. *The Journal of Neuroscience: The Official Journal of the Society for Neuroscience*, *37*(5), 1056–1061. https://doi.org/10.1523/JNEUROSCI.1706-16.2016

Kanwisher, N., McDermott, J., & Chun, M. M. (1997). The fusiform face area: A module in human extrastriate cortex specialized for face perception. *J Neurosci*, *17*(11), 4302–4311. https://doi.org/10.1523/jneurosci.17-11-04302.1997

Kay, K. N., Weiner, K. S., & Grill-Spector, K. (2015). Attention reduces spatial uncertainty in human ventral temporal cortex. *Current Biology*, *25*(5), 595–600. https://doi.org/10.1016/j.cub.2014.12.050

Kietzmann, T. C., Swisher, J. D., König, P., & Tong, F. (2012). Prevalence of selectivity for mirror-symmetric views of faces in the ventral and dorsal visual pathways. *The Journal of Neuroscience: The Official Journal of the Society for Neuroscience*, *32*(34), 11763–11772. https://doi.org/10.1523/JNEUROSCI.0126-12.2012

Kriegeskorte, N., Mur, M., Ruff, D. A., Kiani, R., Bodurka, J., Esteky, H., Tanaka, K., & Bandettini, P. A. (2008). Matching categorical object representations in inferior temporal cortex of man and monkey. *Neuron*, *60*(6), 1126–1141. https://doi.org/10.1016/j.neuron.2008.10.043

Lyu, I., Bao, S., Hao, L., Yao, J., Miller, J. A., Voorhies, W., Taylor, W. D., Bunge, S. A., Weiner, K. S., & Landman, B. A. (2021). Labeling lateral prefrontal sulci using spherical data augmentation and context-aware training. *NeuroImage*, *229*, 117758. https://doi.org/10.1016/j.neuroimage.2021.117758

Maher, S., Ekstrom, T., Ongur, D., Levy, D. L., Norton, D. J., Nickerson, L. D., & Chen, Y. (2019). Functional disconnection between the visual cortex and right fusiform face area in schizophrenia. *Schizophrenia Research*, *209*, 72–79. https://doi.org/10.1016/j.schres.2019.05.016

Mahon, B. Z., & Caramazza, A. (2009). Concepts and categories: A cognitive neuropsychological perspective. *Annu Rev Psychol*, *60*, 27–51. https://doi.org/10.1146/annurev.psych.60.110707.163532

962 Malach, R., Levy, I., & Hasson, U. (2002). The topography of high-order human object
963 areas. *Trends Cogn Sci*, *6*(4), 176–184. https://doi.org/10.1016/s1364-
964 6613(02)01870-3
965 Martin, A. (2007). The representation of object concepts in the brain. *Annu Rev Psychol*,
966 *58*, 25–45. https://doi.org/10.1146/annurev.psych.57.102904.190143
967 McGugin, R. W., Gatenby, J. C., Gore, J. C., & Gauthier, I. (2012). High-resolution
968 imaging of expertise reveals reliable object selectivity in the fusiform face area
969 related to perceptual performance. *Proc. Natl. Acad. Sci. U. S. A.*, *109*(42),
970 17063–17068. https://doi.org/10.1073/pnas.1116333109
971 McGugin, R. W., Newton, A. T., Gore, J. C., & Gauthier, I. (2014). Robust expertise
972 effects in right FFA. *Neuropsychologia*, *63*, 135–144.
973 https://doi.org/10.1016/j.neuropsychologia.2014.08.029
974 McGugin, R. W., Van Gulick, A. E., & Gauthier, I. (2016). Cortical thickness in fusiform
975 face area predicts face and object recognition performance. *Journal of Cognitive*
976 *Neuroscience*, *28*(2), 282–294. https://doi.org/10.1162/jocn_a_00891
977 McGugin, R. W., Van Gulick, A. E., Tamber-Rosenau, B. J., Ross, D. A., & Gauthier, I.
978 (2015). Expertise effects in face-selective areas are robust to clutter and diverted
979 attention, but not to competition. *Cerebral Cortex*, *25*(9), 2610–2622.
980 https://doi.org/10.1093/cercor/bhu060
981 Nasr, S., Liu, N., Devaney, K. J., Yue, X., Rajimehr, R., Ungerleider, L. G., & Tootell, R.
982 B. (2011). Scene-selective cortical regions in human and nonhuman primates. *J*
983 *Neurosci*, *31*(39), 13771–13785. https://doi.org/10.1523/JNEUROSCI.2792-
984 11.2011
985 Natu, V. S., Barnett, M. A., Hartley, J., Gomez, J., Stigliani, A., & Grill-Spector, K.
986 (2016). Development of neural sensitivity to face identity correlates with
987 perceptual discriminability. *The Journal of Neuroscience: The Official Journal of*
988 *the Society for Neuroscience*, *36*(42), 10893–10907.
989 https://doi.org/10.1523/JNEUROSCI.1886-16.2016
990 Natu, V. S., Gomez, J., Barnett, M., Jeska, B., Kirilina, E., Jaeger, C., Zhen, Z., Cox, S.,
991 Weiner, K. S., Weiskopf, N., & Grill-Spector, K. (2019). Apparent thinning of
992 human visual cortex during childhood is associated with myelination.

Proceedings of the National Academy of Sciences, *116*(41), 20750–20759. https://doi.org/10.1073/pnas.1904931116

Nordt, M., Gomez, J., Natu, V. S., Rezai, A. A., Finzi, D., Kular, H., & Grill-Spector, K. (2021). Cortical recycling in high-level visual cortex during childhood development. *Nature Human Behaviour*, *5*(12), 1686–1697. https://doi.org/10.1038/s41562-021-01141-5

Park, J., Carp, J., Kennedy, K. M., Rodrigue, K. M., Bischof, G. N., Huang, C.-M., Rieck, J. R., Polk, T. A., & Park, D. C. (2012). Neural broadening or neural attenuation? Investigating age-related dedifferentiation in the face network in a large lifespan sample. *The Journal of Neuroscience: The Official Journal of the Society for Neuroscience*, *32*(6), 2154–2158. https://doi.org/10.1523/JNEUROSCI.4494-11.2012

Parvizi, J., Jacques, C., Foster, B. L., Withoft, N., Rangarajan, V., Weiner, K. S., & Grill-Spector, K. (2012). Electrical stimulation of human fusiform face-selective regions distorts face perception. *Journal of Neuroscience*, *32*(43), 14915–14920. https://doi.org/10.1523/JNEUROSCI.2609-12.2012

Pinsk, M. A., Arcaro, M., Weiner, K. S., Kalkus, J. F., Inati, S. J., Gross, C. G., & Kastner, S. (2009). Neural representations of faces and body parts in macaque and human cortex: A comparative FMRI study. *J Neurophysiol*, *101*(5), 2581–2600. https://doi.org/10.1152/jn.91198.2008

Pitcher, D., Dilks, D. D., Saxe, R. R., Triantafyllou, C., & Kanwisher, N. (2011). Differential selectivity for dynamic versus static information in face-selective cortical regions. *NeuroImage*, *56*(4), 2356–2363. https://doi.org/10.1016/j.neuroimage.2011.03.067

Pitcher, D., & Ungerleider, L. G. (2021). Evidence for a third visual pathway specialized for social perception. *Trends in Cognitive Sciences, 25*(2), 100–110. https://doi.org/10.1016/j.tics.2020.11.006

Poldrack, R. A., Laumann, T. O., Koyejo, O., Gregory, B., Hover, A., Chen, M.-Y., Gorgolewski, K. J., Luci, J., Joo, S. J., Boyd, R. L., Hunicke-Smith, S., Simpson, Z. B., Caven, T., Sochat, V., Shine, J. M., Gordon, E., Snyder, A. Z., Adeyemo, B., Petersen, S. E., … Mumford, J. A. (2015). Long-term neural and physiological

phenotyping of a single human. *Nature Communications*, *6*(1), 8885. https://doi.org/10.1038/ncomms9885

Price, C. J. & Friston, K. J. (2002). Degeneracy and cognitive anatomy. *Trends in Cognitive Sciences*, *6*(10), 416-421. https://doi.org/10.1016/s1364-6613(02)01976-9

Rangarajan, V., Hermes, D., Foster, B. L., Weiner, K. S., Jacques, C., Grill-Spector, K., & Parvizi, J. (2014). Electrical stimulation of the left and right human fusiform gyrus causes different effects in conscious face perception. *Journal of Neuroscience*, *34*(38), 12828–12836. https://doi.org/10.1523/JNEUROSCI.0527-14.2014

Robinson, E. C., Jbabdi, S., Glasser, M. F., Andersson, J., Burgess, G. C., Harms, M. P., Smith, S. M., Van Essen, D. C., & Jenkinson, M. (2014). MSM: A new flexible framework for Multimodal Surface Matching. *NeuroImage*, *100*, 414–426. https://doi.org/10.1016/j.neuroimage.2014.05.069

Rosenke, M., Davidenko, N., Grill-Spector, K., & Weiner, K. S. (2020). Combined neural tuning in human ventral temporal cortex resolves the perceptual ambiguity of morphed 2D images. *Cerebral Cortex*, *30*(9), 4882–4898. https://doi.org/10.1093/cercor/bhaa081

Rosenke, M., van Hoof, R., van den Hurk, J., Grill-Spector, K., & Goebel, R. (2021). A probabilistic functional atlas of human occipito-temporal visual cortex. *Cerebral Cortex*, *31*(1), 603–619. https://doi.org/10.1093/cercor/bhaa246

Rossion, B. (2008). Constraining the cortical face network by neuroimaging studies of acquired prosopagnosia. *NeuroImage*, *40*(2), 423–426. https://doi.org/10.1016/j.neuroimage.2007.10.047

Rossion, B., Caldara, R., Seghier, M., Schuller, A., Lazeyras, F., & Mayer, E. (2003). A network of occipito-temporal face-sensitive areas besides the right middle fusiform gyrus is necessary for normal face processing. *Brain*, *126*(11), 2381–2395. https://doi.org/10.1093/brain/awg241

Rossion, B., Jacques, C., & Jonas, J. (2018). Mapping face categorization in the human ventral occipitotemporal cortex with direct neural intracranial recordings. *Annals*

of the New York Academy of Sciences, 1426(1), 5-24. https://doi.org/10.1111/nyas.13596

Saxe, R., Brett, M., & Kanwisher, N. (2006). Divide and conquer: A defense of functional localizers. *NeuroImage*, *30*(4), 1088–1096. https://doi.org/10.1016/j.neuroimage.2005.12.062

Schalk, G., Kapeller, C., Guger, C., Ogawa, H., Hiroshima, S., Lafer-Sousa, R., Saygin, Z. M., Kamada, K., & Kanwisher, N. (2017). Facephenes and rainbows: Causal evidence for functional and anatomical specificity of face and color processing in the human brain. *Proceedings of the National Academy of Sciences of the United States of America*, *114*(46), 12285–12290. https://doi.org/10.1073/pnas.1713447114

Scherf, K. S., Behrmann, M., & Dahl, R. E. (2012). Facing changes and changing faces in adolescence: A new model for investigating adolescent-specific interactions between pubertal, brain and behavioral development. *Developmental Cognitive Neuroscience*, *2*(2), 199–219. https://doi.org/10.1016/j.dcn.2011.07.016

Scherf, K. S., Behrmann, M., Humphreys, K., & Luna, B. (2007). Visual category-selectivity for faces, places and objects emerges along different developmental trajectories. *Developmental Science*, *10*(4), F15-30. https://doi.org/10.1111/j.1467-7687.2007.00595.x

Scherf, K. S., Elbich, D. B., & Motta-Mena, N. V. (2017). Investigating the influence of biological sex on the behavioral and neural basis of face recognition. *ENeuro*, *4*(3), ENEURO.0104-17.2017. https://doi.org/10.1523/ENEURO.0104-17.2017

Scherf, K. S., Thomas, C., Doyle, J., & Behrmann, M. (2014). Emerging structure-function relations in the developing face processing system. *Cerebral Cortex*, *24*(11), 2964–2980. https://doi.org/10.1093/cercor/bht152

Schrouff, J., Raccah, O., Baek, S., Rangarajan, V., Salehi, S., Mourão-Miranda, J., Helili, Z., Daitch, A. L., & Parvizi, J. (2020). Fast temporal dynamics and causal relevance of face processing in the human temporal cortex. *Nature Communications*, *11*(1), 656. https://doi.org/10.1038/s41467-020-14432-8

Silson, E. H., Groen, I. I. A., Kravitz, D. J., & Baker, C. I. (2016). Evaluating the correspondence between face-, scene-, and object-selectivity and retinotopic

organization within lateral occipitotemporal cortex. *Journal of Vision*, *16*(6), 14. https://doi.org/10.1167/16.6.14

Silson, E. H., Reynolds, R. C., Kravitz, D. J., & Baker, C. I. (2018). Differential sampling of visual space in ventral and dorsal early visual cortex. *The Journal of Neuroscience: The Official Journal of the Society for Neuroscience*, *38*(9), 2294–2303. https://doi.org/10.1523/JNEUROSCI.2717-17.2018

Smith, S. M., Beckmann, C. F., Andersson, J., Auerbach, E. J., Bijsterbosch, J., Douaud, G., Duff, E., Feinberg, D. A., Griffanti, L., Harms, M. P., Kelly, M., Laumann, T., Miller, K. L., Moeller, S., Petersen, S., Power, J., Salimi-Khorshidi, G., Snyder, A. Z., Vu, A. T., … WU-Minn HCP Consortium. (2013). Resting-state fMRI in the Human Connectome Project. *NeuroImage*, *80*, 144–168. https://doi.org/10.1016/j.neuroimage.2013.05.039

Stigliani, A., Jeska, B., & Grill-Spector, K. (2019). Differential sustained and transient temporal processing across visual streams. *PLOS Computational Biology*, *15*(5), e1007011. https://doi.org/10.1371/journal.pcbi.1007011

Stigliani, A., Weiner, K. S., & Grill-Spector, K. (2015). Temporal processing capacity in high-level visual cortex is domain specific. *The Journal of Neuroscience: The Official Journal of the Society for Neuroscience*, *35*(36), 12412–12424. https://doi.org/10.1523/JNEUROSCI.4822-14.2015

Tarr, M. J., & Gauthier, I. (2000). FFA: a flexible fusiform area for subordinate-level visual processing automatized by expertise. *Nat Neurosci*, *3*(8), 764–769. https://doi.org/10.1038/77666

Tsao, D. Y., & Livingstone, M. S. (2008). Mechanisms of face perception. *Annu Rev Neurosci*, *31*, 411–437. https://doi.org/10.1146/annurev.neuro.30.051606.094238

Tsao, D. Y., Schweers, N., Moeller, S., & Freiwald, W. A. (2008). Patches of face-selective cortex in the macaque frontal lobe. *Nat Neurosci*, *11*(8), 877–879. https://doi.org/10.1038/nn.2158

Uğurbil, K., Xu, J., Auerbach, E. J., Moeller, S., Vu, A. T., Duarte-Carvajalino, J. M., Lenglet, C., Wu, X., Schmitter, S., Van de Moortele, P. F., Strupp, J., Sapiro, G., De Martino, F., Wang, D., Harel, N., Garwood, M., Chen, L., Feinberg, D. A., Smith, S. M., … WU-Minn HCP Consortium. (2013). Pushing spatial and

temporal resolution for functional and diffusion MRI in the Human Connectome Project. *NeuroImage*, *80*, 80–104. https://doi.org/10.1016/j.neuroimage.2013.05.012

Van Essen, D. C., & Glasser, M. F. (2018). Parcellating cerebral cortex: How invasive animal studies inform noninvasive mapmaking in humans. *Neuron*, *99*(4), 640–663. https://doi.org/10.1016/j.neuron.2018.07.002

Van Essen, D. C., Smith, S. M., Barch, D. M., Behrens, T. E. J., Yacoub, E., & Ugurbil, K. (2013). The WU-Minn Human Connectome Project: An overview. *NeuroImage*, *80*, 62–79. https://doi.org/10.1016/j.neuroimage.2013.05.041

Weiner, K. S. (2019). The mid-fusiform sulcus (sulcus sagittalis gyri fusiformis). *Anatomical Record (Hoboken, N.J.: 2007)*, *302*(9), 1491–1503. https://doi.org/10.1002/ar.24041

Weiner, K. S., Barnett, M. A., Lorenz, S., Caspers, J., Stigliani, A., Amunts, K., Zilles, K., Fischl, B., & Grill-Spector, K. (2017). The cytoarchitecture of domain-specific regions in human high-level visual cortex. *Cerebral Cortex*, *27*(1), 146–161. https://doi.org/10.1093/cercor/bhw361

Weiner, K. S., Golarai, G., Caspers, J., Chuapoco, M. R., Mohlberg, H., Zilles, K., Amunts, K., & Grill-Spector, K. (2014). The mid-fusiform sulcus: A landmark identifying both cytoarchitectonic and functional divisions of human ventral temporal cortex. *NeuroImage*, *84*, 453–465. https://doi.org/10.1016/j.neuroimage.2013.08.068

Weiner, K. S., & Grill-Spector, K. (2010). Sparsely-distributed organization of face and limb activations in human ventral temporal cortex. *NeuroImage*, *52*(4), 1559–1573. https://doi.org/10.1016/j.neuroimage.2010.04.262

Weiner, K. S., & Grill-Spector, K. (2013). Neural representations of faces and limbs neighbor in human high-level visual cortex: Evidence for a new organization principle. *Psychological Research*, *77*(1), 74–97. https://doi.org/10.1007/s00426-011-0392-x

Weiner, K. S., Jonas, J., Gomez, J., Maillard, L., Brissart, H., Hossu, G., Jacques, C., Loftus, D., Colnat-Coulbois, S., Stigliani, A., Barnett, M. A., Grill-Spector, K., & Rossion, B. (2016). The face-processing network is resilient to focal resection of

human visual cortex. *The Journal of Neuroscience: The Official Journal of the Society for Neuroscience*, *36*(32), 8425–8440. https://doi.org/10.1523/JNEUROSCI.4509-15.2016

Weiner, K. S., Sayres, R., Vinberg, J., & Grill-Spector, K. (2010). fMRI-adaptation and category selectivity in human ventral temporal cortex: Regional differences across time scales. *Journal of Neurophysiology*, *103*(6), 3349–3365. https://doi.org/10.1152/jn.01108.2009

Wilmer, J. B., Germine, L., Chabris, C. F., Chatterjee, G., Williams, M., Loken, E., Nakayama, K., & Duchaine, B. (2010). Human face recognition ability is specific and highly heritable. *Proceedings of the National Academy of Sciences of the United States of America*, *107*(11), 5238–5241. https://doi.org/10.1073/pnas.0913053107

Wu, C., Zhen, Z., Huang, L., Huang, T., & Liu, J. (2020). COMT-polymorphisms modulated functional profile of the fusiform face area contributes to face-specific recognition ability. *Scientific Reports*, *10*(1), 2134. https://doi.org/10.1038/s41598-020-58747-4

Zhen, Z., Yang, Z., Huang, L., Kong, X., Wang, X., Dang, X., Huang, Y., Song, Y., & Liu, J. (2015). Quantifying interindividual variability and asymmetry of face-selective regions: A probabilistic functional atlas. *NeuroImage*, *113*, 13–25. https://doi.org/10.1016/j.neuroimage.2015.03.010

Zhu, Q., Song, Y., Hu, S., Li, X., Tian, M., Zhen, Z., Dong, Q., Kanwisher, N., & Liu, J. (2010). Heritability of the specific cognitive ability of face perception. *Current Biology*, *20*(2), 137–142. https://doi.org/10.1016/j.cub.2009.11.067